

June 1982

ANALYSES OF CAPSULE CR3-B  
FLORIDA POWER CORPORATION  
CRYSTAL RIVER UNIT 3

- Reactor Vessel Materials Surveillance Program -

**Babcock & Wilcox**

a McDermott company

8502200322 850214  
PDR ADOCK 05000302  
P PDR

June 1982

ANALYSES OF CAPSULE CR3-B  
FLORIDA POWER CORPORATION  
CRYSTAL RIVER UNIT 3

— Reactor Vessel Materials Surveillance Program —

by

A. L. Lowe, Jr., PE  
M. S. Abraham  
C. E. Harris  
J. K. Schmotzer  
C. L. Whitmarsh

B&W Contract No. 595-7030-65

BABCOCK & WILCOX  
Nuclear Power Group  
Nuclear Power Generation Division  
P. O. Box 1260  
Lynchburg, Virginia 24505

## 1. INTRODUCTION

This report describes the results of the examination of the first capsule of the Florida Power Corporation's Crystal River Unit 3 reactor vessel surveillance program. The capsule was removed and examined after the first year of operation. (Capsule removed during March 1978 outage.) | 1

The objective of the program is to monitor the effects of neutron irradiation on the tensile and impact properties of reactor pressure vessel materials under actual operating conditions. The surveillance program for Crystal River Unit 3 was designed and furnished by Babcock & Wilcox as described in BAW-10100A.<sup>1</sup> The program was designed in accordance with the requirements of Appendix H to 10 CFR Part 50 and ASTM specification E185-73 and was planned to monitor the effects of neutron irradiation on the reactor vessel material for the 40-year design life of the reactor pressure vessel. The future operating limitations established after the evaluation of the surveillance capsule are also in accordance with the requirement of 10 CFR 50, Appendixes G and H. The recommended operating period was extended to eight effective full power years as a result of the first capsule evaluation.

This revision addresses the affects of the change in fuel management - a longer fuel cycle and higher power level, which result in a lower estimated EOL fluence. | 1

## 2. BACKGROUND

The ability of the reactor pressure vessel to resist fracture is the primary factor in ensuring the safety of the primary system in light water cooled reactors. The beltline region of the reactor vessel is the most critical region of the vessel because it is exposed to neutron irradiation. The general effects of fast neutron irradiation on the mechanical properties of such low-alloy ferritic steels as SA533, Grade B, used in the fabrication of the Crystal River River Unit 3 reactor vessel are well characterized and documented in the literature. The low-alloy ferritic steels used in the beltline region of reactor vessels exhibit an increase in ultimate and yield strength properties with a corresponding decrease in ductility after irradiation. In reactor pressure vessel steels, the most serious mechanical property change is the increase in temperature for the transition from brittle to ductile fracture accompanied by a reduction in the upper shelf impact toughness.

Appendix G to 10 CFR 50, "Fracture Toughness Requirements," specifies minimum fracture toughness requirements for the ferritic materials of the pressure-retaining components of the reactor coolant pressure boundary (RCPB) of water-cooled power reactors and provides specific guidelines for determining the pressure-temperature limitations on operation of the RCPB. The toughness and operational requirements are specified to provide adequate safety margins during any condition of normal operation, including anticipated operational occurrences and system hydrostatic tests, to which the pressure boundary may be subjected over its service lifetime. Although the requirements of Appendix G to 10 CFR 50 became effective on August 13, 1973, the requirements are applicable to all boiling and pressurized water-cooled nuclear power reactors, including those under construction or in operation on the effective date.

Appendix H to 10 CFR 50, "Reactor Vessel Materials Surveillance Program Requirements," defines the material surveillance program required to monitor changes in the fracture toughness properties of ferritic materials in the reactor vessel beltline region of water-cooled reactors resulting from exposure

to neutron irradiation and the thermal environment. Fracture toughness test data are obtained from material specimens withdrawn periodically from the reactor vessel. These data will permit determination of the conditions under which the vessel can be operated with adequate safety margins against fracture throughout its service life.

A method for guarding against brittle fracture in reactor pressure vessels is described in Appendix G to the ASME Boiler and Pressure Vessel Code, Section III. This method utilizes fracture mechanics concepts and the reference nil-ductility temperature,  $RT_{NDT}$ , which is defined as the greater of the drop weight nil-ductility transition temperature (per ASTM E-208) or the temperature that is 60F below that at which the material exhibits 50 ft-lb and 35 mils lateral expansion. The  $RT_{NDT}$  of a given material is used to index that material to a reference stress intensity factor curve ( $K_{IR}$  curve), which appears in Appendix G of ASME Section III. The  $K_{IR}$  curve is a lower bound of dynamic, static, and crack arrest fracture toughness results obtained from several heats of pressure vessel steel. When a given material is indexed to the  $K_{IR}$  curve, allowable stress intensity factors can be obtained for this material as a function of temperature. Allowable operating limits can then be determined using these allowable stress intensity factors.

The  $RT_{NDT}$  and, in turn, the operating limits of a nuclear power plant, can be adjusted to account for the effects of radiation on the properties of the reactor vessel materials. The radiation embrittlement and the resultant changes in mechanical properties of a given pressure vessel steel can be monitored by a surveillance program in which a surveillance capsule containing prepared specimens of the reactor vessel materials is periodically removed from the operating nuclear reactor and the specimens tested. The increase in the Charpy V-notch 50-ft-lb temperature, or the increase in the 35 mils of lateral expansion temperature, whichever results in the larger temperature shift due to irradiation, is added to the original  $RT_{NDT}$  to adjust it for radiation embrittlement. This adjusted  $RT_{NDT}$  is used to index the material to the  $K_{IR}$  curve, which, in turn is used to set operating limits for the nuclear power plant. These new limits take into account the effects of irradiation on the reactor vessel materials.

### 3. SURVEILLANCE PROGRAM DESCRIPTION

The surveillance program comprises six surveillance capsules designed to monitor the effects of neutron and thermal environment on the materials of the reactor pressure vessel core region. The capsules, which were inserted into the reactor vessel before initial plant startup, were positioned inside the reactor vessel between the thermal shield and the vessel wall at the locations shown in Figure 3-1. The six capsules, placed two in each holder tube, are positioned near the peak axial and azimuthal neutron flux. BAW-10100A includes a full description of capsule locations and design.<sup>1</sup>

Capsule CR3-B was removed during the first refueling shutdown of Crystal River Unit 3. This capsule contained Charpy V-notch impact and tensile specimens fabricated of SA533, Grade B Class 1, weld metal, and weld metal compact fracture specimens. The specimens contained in the capsule are described in Table 3-1, and the chemistry and heat treatment of the surveillance material in capsule CR-3B are described in Table 3-2.

All test specimens were machined from the 1/4-thickness location of the plates. Charpy V-notch and tensile specimens from the vessel material were oriented with their longitudinal axes parallel to the principal rolling direction of the plate; specimens were also oriented transverse to the principal rolling direction. Capsule CR3-B contained dosimeter wires, described as follows:

<u>Dosimeter wire</u>	<u>Shielding</u>
U-Al alloy	Cd-Ag alloy
Np-Al alloy	Cd-Ag alloy
Nickel	Cd-Ag alloy
0.56 wt % Co-Al alloy	Cd
0.56 wt % Co-Al alloy	None
Fe	None

Thermal monitors of low-melting eutectic alloys were included in the capsule. The eutectic alloys and their melting points are as follows:

<u>Alloy</u>	<u>Melting point, F</u>
90% Pb, 5% Ag, 5% Sn	558
97.5% Pb, 2.5% Ag	580
97.5% Pb, 1.5% Ag, 1.0% Sn	588
Lead	621
Cadmium	610

Table 3-1. Specimens in Surveillance Capsule CR3-B

<u>Material description</u>	<u>Number of test specimens</u>		
	<u>Tension</u>	<u>CVN impact</u>	<u>1/2 T compact tension</u> <sup>(a)</sup>
Weld metal	2	12	8
Weld-HAZ			
Heat NN, transverse	--	12	--
Base metal			
Heat NN, transverse	<u>2</u>	<u>12</u>	<u>--</u>
Total per capsule	4	36	8

(a) Compact tension specimens pre-cracked per ASTM E399-72.

Table 3-2. Chemistry and Heat Treatment  
of Surveillance Materials

Chemical Analysis

<u>Element</u>	<u>Heat C-4344-1</u>	<u>Weld metal WF-209-1<sup>(a)</sup></u>	<u>Weld metal WF-209-1<sup>(b)</sup></u>
C	0.23	0.08	0.11
Mn	1.30	1.65	1.57
P	0.008	0.021	0.018
S	0.016	0.013	0.009
Si	0.22	1.00	0.54
Ni	0.54	0.10	0.61
Mo	0.55	0.45	0.43
Cu	0.20	0.39	0.36

Heat Treatment

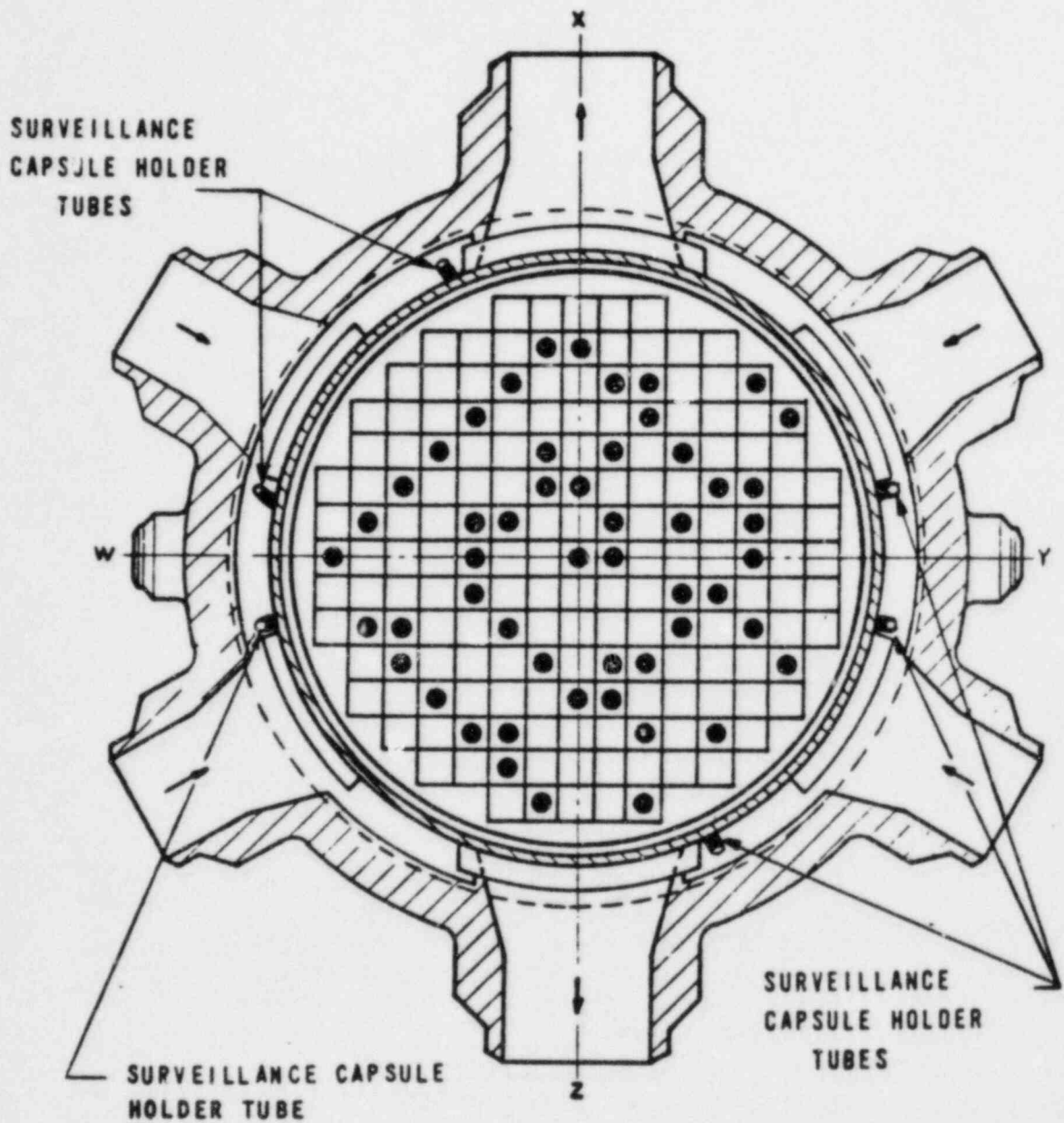
<u>Heat No.</u>	<u>Temp, F</u>	<u>Time, h</u>	<u>Cooling</u>
C-4344-1	1650-1700	9	Water quench
	1180	4.5	Air cooled
	1100-1150	60.0	Furnace cooled
WF-209-1	1100-1150	48.0	Furnace cooled

(a) The weld metal used to fabricate the Charpy and tensile specimens has been identified as "atypical" weld metal, as described in BAW-10144, February 1980.<sup>5</sup> The compact fracture specimens are fabricated from the designated weld metal.

(b) The weld metal used to fabricate the compact fracture specimens has been identified as from the designated weld metal, as described in BAW-10144, February 1980.<sup>5</sup>



Figure 3-1. Reactor Vessel Cross Section



#### 4. PREIRRADIATION TESTS

Unirradiated material was evaluated for two purposes: (1) to establish a baseline of data to which irradiated properties data could be referenced, and (2) to determine those materials properties to the extent practical from available material, as required for compliance with Appendixes G and H to 10 CFR 50.

##### 4.1. Tensile Tests

Tensile specimens were fabricated from the reactor vessel shell course plate and weld metal. The subsized specimens were 4.25 inches long with a reduced section 1.750 inches long by 0.357 inch in diameter. They were tested on a 55,000-lb-load capacity universal test machine at a crosshead speed of 0.050 inch per minute. A 4-pole extension device with a strain gaged extensometer was used to determine the 0.2% yield point. Test conditions were in accordance with the applicable requirements of ASTM A370-72. For each material type and/or condition, six specimens in groups of three were tested at both room temperature and 580F. The tension-compression load cell used had a certified accuracy of better than  $\pm 0.5\%$  of full scale (25,000 lb). All test data for the preirradiation tensile specimens are given in Appendix B.

##### 4.2. Impact Tests

Charpy V-notch impact tests were conducted in accordance with the requirements of ASTM Standard Methods A370-72 and E23-72 on an impact tester certified to meet Watertown standards. Test specimens were of the Charpy V-notch type, which were nominally 0.394 inch square and 2.165 inches long.

Prior to testing, specimens were temperature-controlled in liquid immersion baths, capable of covering the temperature range from -85 to +550F. Specimens were removed from the baths and positioned in the test frame anvil with tongs specifically designed for the purpose. The pendulum (hammer) was released manually, allowing the specimens to be broken within 5 seconds from their removal from the temperature baths.

Impact test data for the unirradiated baseline reference materials are presented in Appendix C. Tables C-1 through C-5 contain the basis data which are plotted in Figures C-1 through C-5.

#### 4.3. Compact Fracture Tests

The compact fracture specimens fabricated from the weld metal, which were a part of the capsule specimen inventory, were not tested because of the lack of a recognized testing procedure. These specimens will be kept in bonded storage until an acceptable test procedure is developed. The results of the testing of these specimens will be the subject of a separate report.

## 5. POST-IRRADIATION TESTS

### 5.1. Thermal Monitors

Surveillance capsule CR3-B contained three temperature monitor holder tubes, each containing five fusible alloys with different melting points ranging from 558 to 621F. All the thermal monitors at 558 and 580F had melted, while those at 588, 610, and 621F remained in their original configuration as initially placed in the capsule. From these data it was concluded that the irradiated specimens had been exposed to a maximum temperature in the range of 580 to less than 588F during the reactor vessel operating period. There appeared to be no significant temperature gradient along the capsule length.

### 5.2. Tensile Test Results

The results of the post-irradiation tensile tests are presented in Table 5-1. Tests were performed on specimens at both room temperature and 580F using the same test procedures and techniques used to test the unirradiated specimens (section 4.1). In general, the ultimate strength and yield strength of the material increased slightly with a corresponding slight decrease in ductility; both effects were the result of neutron radiation damage. The type of behavior observed and the degree to which the material properties changed is within the range of changes to be expected for the radiation environment to which the specimens were exposed.

The results of the preirradiation tensile tests are presented in Appendix B.

### 5.3. Charpy V-Notch Impact Test Results

The test results from the irradiated Charpy V-notch specimens of the reactor vessel beltline material and the correlation monitor material are presented in Tables 5-2 through 5-4 and Figures 5-1 through 5-3. The test procedures and techniques were the same as those used to test the unirradiated specimens (section 4.2). The data show that the material exhibited a sensitivity to irradiation within the values predicted from its chemical composition and the fluence to which it was exposed.

The results of the preirradiation Charpy V-notch impact test are given in Appendix C.

Table 5-1. Tensile Properties of Capsule CR3-B Base Metal and Weld Metal Irradiated to 1.0E18 nvt (>1 MeV)

Specimen No.	Test temp, F	Strength, psi		Elongation, %		Red'n in area, %
		Yield	Ult.	Unif	Total	
<u>Base Metal, Transverse</u>						
NN-620	RT	78,125	100,000	E.S.	27	61
NN-615	580	69,375	95,625	10	21	49
<u>Weld Metal</u>						
PP-007	RT	83,125	98,750	12	27	62
PP-017	580	69,375	90,625	12	25	53

Table 5-2. Charpy Impact Data From Capsule CR3-B Base Metal Irradiated to 1.0E18 (> 1 MeV)

Specimen No.	Test temp, F	Absorbed energy, ft-lb	Lateral expansion, 10 <sup>-3</sup> in.	Shear fracture, %
<u>Base Metal, Transverse</u>				
NN-689	20	24	16	10
NN-605	50	34	30	10
NN-658	70	33	36	30
NN-685	85	37	32	30
NN-641	100	43	39	30
NN-646	120	56	44	30
NN-650	140	59	54	70
NN-613	170	66	58	100
NN-608	190	93	73	100
NN-616	210	89	76	100
NN-630	260	89	73	100
NN-632	300	88	74	100

Table 5-3. Charpy Impact Data From Capsule CR3-B  
Heat-Affected Zone Metal Irradiated  
to 8.4E17 (>1 MeV)

Specimen No.	Test temp, F	Absorbed energy, ft-lb	Lateral expansion, 10 <sup>-3</sup> in.	Shear fracture, %
<u>Heat-Affected Zone, Transverse</u>				
NN-392	20	23	14	20
NN-372	50	28	21	30
NN-365	70	39	33	28
NN-366	100	60	50	88
NN-377	120	51	43	100
NN-352	140	44	36	30
NN-381	170	60	56	100
NN-375	210	74	63	100
NN-389	260	66	62	100
NN-374	285	79	67	100
NN-383	320	84	67	100
NN-380	360	74	65	100

Table 5-4. Charpy Impact Data From Capsule CR3-B  
Weld Metal Irradiated to 1.17E18 n/cm<sup>2</sup>  
(>1 MeV)

Specimen No.	Test temp, F	Absorbed energy, ft-lb	Lateral expansion, 10 <sup>-3</sup> in.	Shear fracture, %
PP-092	0	13	11	10
PP-076	35	19	15	10
PP-069	55	27	24	20
PP-059	70	33	30	18
PP-082	95	35	31	30
PP-070	120	48	44	60
PP-091	130	40	38	45
PP-058	140	61	53	100
PP-089	190	70	66	100
PP-077	250	74	68	100
PP-088	285	66	66	100
PP-065	320	70	71	100

Figure 5-1. Charpy Impact Data for Irradiated Base Metal, Transverse Direction

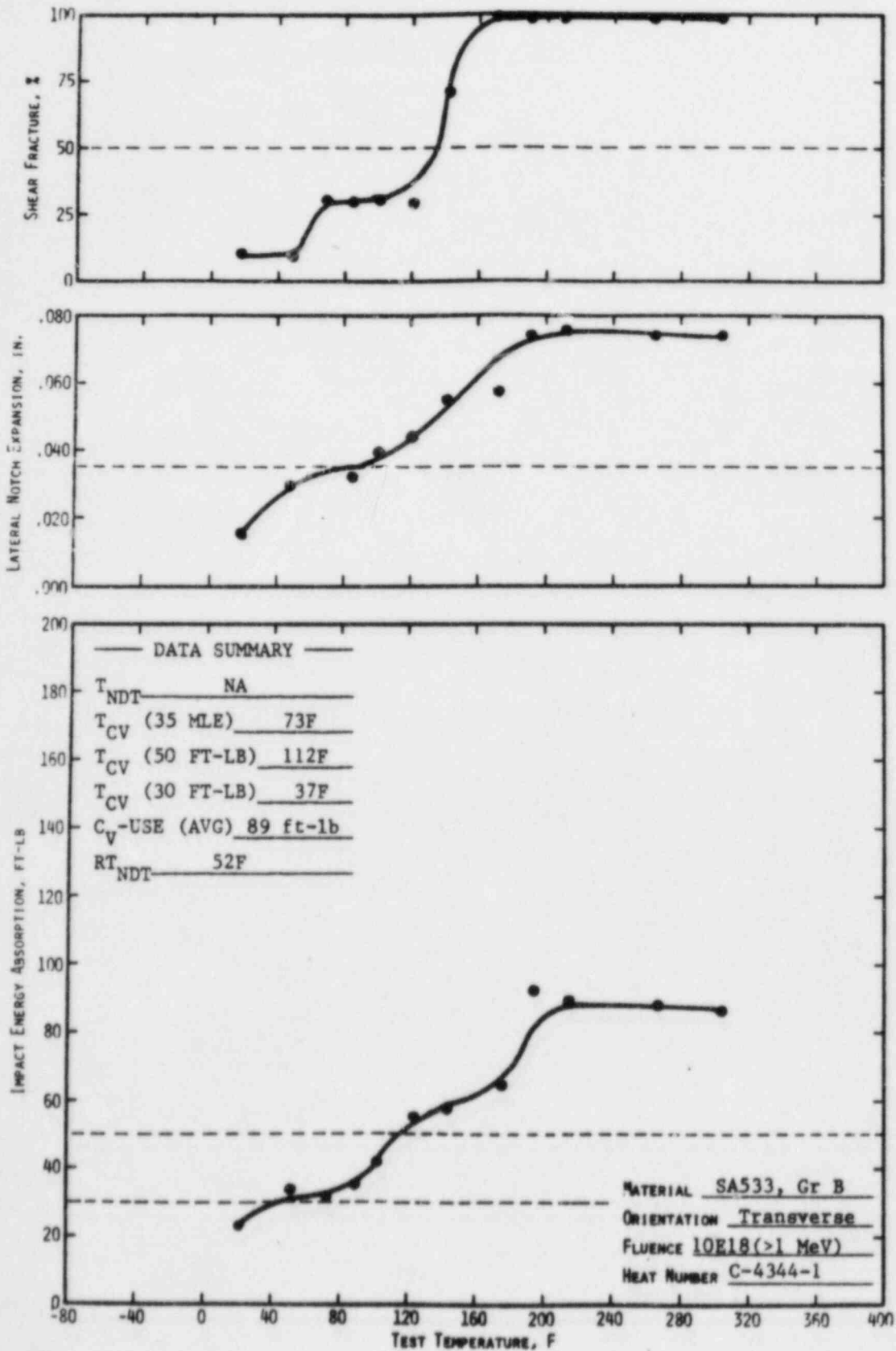


Figure 5-2. Charpy Impact Data for Irradiated Base Metal, Heat-Affected Zone

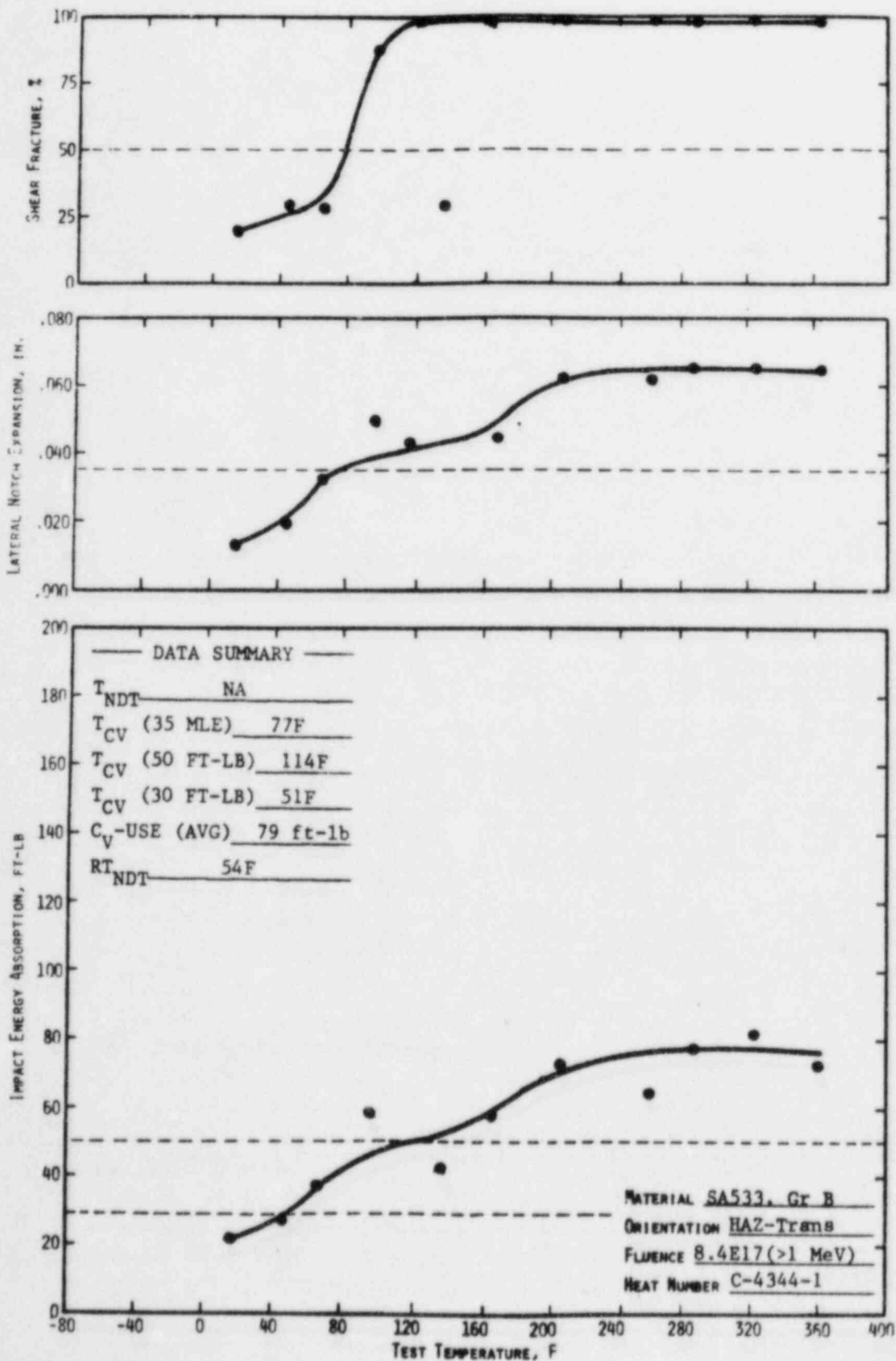
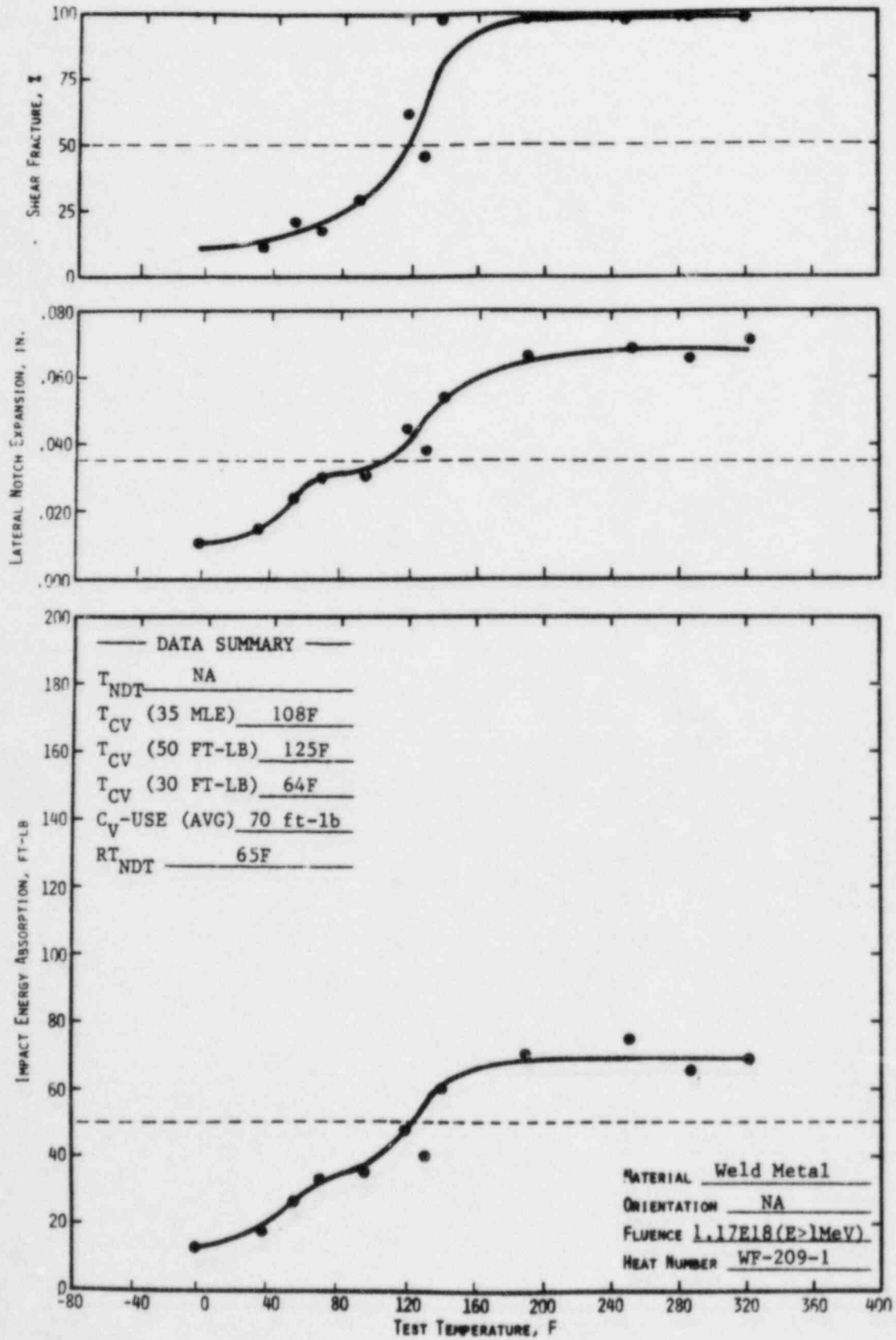




Figure 5-3. Charpy Impact Data for Irradiated Weld Metal



## 6. NEUTRON DOSIMETRY

### 6.1. Introduction

A significant aspect of the surveillance program is to provide a correlation between the neutron fluence above 1 MeV and the radiation-induced property changes noted in the surveillance specimen. To permit such a correlation, activation detectors with reaction thresholds in the energy range of interest were placed in each surveillance capsule. The properties of interest for the detectors are given in Table 6-1.

Because of a long half life of 30 years and an effective energy range of  $>0.5$  MeV, only the measurements of  $^{137}\text{Cs}$  production from fission reactions in  $^{237}\text{Np}$  and  $^{238}\text{U}$  are directly applicable to analytical determinations of fast neutron ( $E > 1$  MeV) fluence during cycle 1. The other dosimeter reactions are useful as corroborating data for shorter time intervals and/or higher energy fluxes. Short-lived isotope activities are representative of reactor conditions over the latter portion of the irradiation period (full cycle) only; whereas reactions with a high threshold energy do not record a significant part of the total fast flux.

The energy-dependent neutron flux is not directly available from activation detectors because the dosimeters record only the integrated effect of the neutron flux on the target material as a function of both irradiation time and neutron energy. To obtain an accurate estimate of the average neutron flux incident upon the detector, the following parameters must be known: the operating history of the reactor, the energy response of the given detector, and the neutron spectrum at the detector location. Of these parameters, the definition of the neutron spectrum is the most difficult to obtain. Essentially, two means are available to obtain the spectrum: iterative unfolding of experimental foil data and analytical methods. Due to a lack of sufficient threshold foil detectors satisfying both the threshold energy and half-life requirements necessary for a surveillance program, iterative unfolding could not be used. This leaves the specification of the neutron spectrum to the analytical method.

## 6.2. Analytical Approach

Energy-dependent neutron fluxes at the detector locations were determined by a discrete ordinates solution of the Boltzmann Transport equation with the two-dimensional code, DOT 35.<sup>2</sup> The CR3 reactor was modelled from the core out to the primary concrete shield in R-theta geometry (based on a plan view along the core midplane and one-eighth core symmetry in the azimuthal dimension). Also included was an explicit model of a holder tube and capsule assembly at the proper location. The CR3-B capsule was positioned 201.84 cm from the core center and 26.9° off-axis. The reactor model contained the following regions: core, liner, bypass coolant, core barrel, inlet coolant, thermal shield, pressure vessel, cavity, and primary concrete shield. Input parameters to the code included a pin by pin time-averaged power distribution, CASK 23E 22-group microscopic neutron cross sections,<sup>3</sup> S<sub>8</sub> order of angular quadrature, and P<sub>3</sub> expansion of the scattering cross section matrix.

Because of computer storage limitations, it was necessary to use two geometric models to cover the distance from core to primary shield. A boundary source output from the initial model A (core through inlet coolant region) was used to "bootstrap" a model B, which included the capsule. Any "shadowing" effect of the pressure vessel by the capsule was determined by running a third model, which represented the model B region of the reactor but without the capsule assembly.

Flux output from the DOT 35 calculations required only an axial distribution adjustment. Thus, fluxes were multiplied by an axial shape factor to account for the capsule elevation. CR3-B was in an upper location which extends from the core midplane upward about 60 cm. This factor was 1.19 for the capsule position and 1.22 for the maximum location on the pressure vessel surface.

The calculation described above provides the neutron flux as a function of energy at the detector position. These calculated data are used in the following equations to obtain the calculated activities used for comparison with the experimental values. The basic equation<sup>4</sup> for the activity D (in μCi/gm) is given as follows:

$$D_1 = \frac{CN}{A_1 \cdot 3.7 \times 10^4} f_1 \int_E \sigma_n(E) \phi(E) \sum_{j=1}^M F_j (1 - e^{-\lambda_1 t_j}) e^{-\lambda_1 (T - \tau_j)} \quad (6-1)$$



where

- $C$  = normalizing constant, ratio of measured to calculated flux,  
 $N$  = Avogadro's number,  
 $A_i$  = atomic weight of target material  $i$ ,  
 $f_i$  = either weight fraction of target isotope in  $n$ th material or fission yield of desired isotope,  
 $\sigma_n(E)$  = group-averaged cross sections for material  $n$ , listed in Table D-3,  
 $\phi(E)$  = group-averaged fluxes calculated by DOT analysis,  
 $F_j$  = fraction of full power during  $j$ th time interval,  $t_j$ ,  
 $\lambda_i$  = decay constant of  $i$ th material,  
 $t_j$  = interval of power history,  
 $T$  = sum of total irradiation time (i.e., residual time in reactor) and wait time between reactor shutdown and counting,  
 $\tau_j$  = cumulative time from reactor startup to end of  $j$ th time period, i.e.,  $\tau_j = \sum_{k=1}^j t_k$ .

The normalizing constant  $C$  can be obtained by equating the right side of equation 6-1 to the measured activity. With  $C$  specified, the neutron fluence greater than 1 MeV can be calculated from

$$\phi(E > 1.0 \text{ MeV}) = C \sum_{E=1}^{15 \text{ MeV}} \phi \sum_{j=1}^M F_j t_j \quad (6-2)$$

where  $M$  is the number of irradiation time intervals; the other values are defined above.

### 6.3. Results

Calculated activities are compared to dosimeter measurements in Table 6-2. The fission wire data indicate about a 20% overprediction of fast flux ( $E > 1 \text{ MeV}$ ) by the analytical model described herein; non-fission wires showed a 30% overprediction. Several factors which could account for this variance — capsule location, reaction cross section spectrum weighting, and measurement techniques — are presently under investigation. Additional dosimetry measurements (not reported here<sup>4</sup>) corroborated the overprediction bias of the analytical-to-measured flux comparison. A safety factor of 1.1 was included in the fluence calculations to provide conservatism in the activity measurements (and therefore capsule and vessel fluence).

Based on a normalization constant of 0.81, an average fast flux for cycle 1 was calculated at the capsule location and the inside surface of the pressure vessel wall. The data (Table 6-4) were converted to fast fluence values of  $1.05 \times 10^{18}$  n/cm<sup>2</sup> at the capsule center and  $2.83 \times 10^{17}$  n/cm<sup>2</sup> at the pressure vessel wall for 268.8 days of cycle 1 at the full power rating of 2452 MWt. Values calculated for the pressure vessel wall (inside surface) refer to the maximum flux, which may be located at a different azimuthal and axial position than the surveillance capsule. In this analysis, the maximum fluence at the pressure vessel occurred at an azimuthal position 7° from a major axis (capsule located at 25.9°) and about 190 cm above the lower active fuel line. This is a function of power distribution in the core. The effect of extending the flux range down to 0.1 MeV was to approximately double the fluence at the capsule and the pressure vessel. Since the same normalization factor of 0.81 is used, additional uncertainty is introduced in this result because none of the dosimeter reactions are effective over this entire energy range.

Based on the surveillance sample analysis for cycle 1, fuel management calculations for reload cores through cycle 5, and estimated future fuel cycles, pressure vessel fluence was predicted up to 32 EFPY (effective full-power years) of operation. These data, which are listed in Table 6-5, are based on the proportionality of vessel fast flux to calculated core leakage flux for cycles 1B through 5. Fuel cycle 5 was assumed to represent an equilibrium cycle for post-cycle operation. This prediction procedure is described in reference 4.

#### 6.4. Summary of Results

1. Calculated activities for fuel cycle 1 exceeded measured activities by 20 to 30%. For the flux range of greater than 1 MeV, a normalizing constant of 0.81 was selected for application to analytical fast flux predictions near the pressure vessel wall.
2. Average fast fluence at the capsule location was  $1.05 \times 10^{18}$  n/cm<sup>2</sup> (E > 1 MeV) after 268.8 days of the first fuel cycle. The maximum value at the pressure vessel wall was calculated to be  $2.8 \times 10^{17}$  n/cm<sup>2</sup>.
3. Extension of the flux range to E > 0.1 MeV tended to approximately double the calculated fluence values.
4. Based on specimen locations within the capsule, the specific fluence was determined for each group of materials (Table 6-6).

Table 6-1. Surveillance Capsule Detectors

<u>Detector reaction</u>	<u>Energy range, MeV</u>	<u>Isotope half-life</u>
$^{54}\text{Fe}(n,p)^{54}\text{Mn}$	>2.5	312 days
$^{58}\text{Ni}(n,p)^{58}\text{Co}$	>2.3	71.3 days
$^{238}\text{U}(n,f)^{137}\text{Cs}$	>1.1	30.2 years
$^{237}\text{Np}(n,f)^{137}\text{Cs}$	>0.5	30.2 years
$^{238}\text{U}(n,f)^{106}\text{Ru}$	>1.1	365 days
$^{237}\text{Np}(n,f)^{106}\text{Ru}$	>0.5	365 days

Table 6-2. Dosimeter Activations

<u>Reaction</u>	<u>Measured activity, (a) <math>\mu\text{Ci/g}</math></u>	<u>Calculated activity, (b) <math>\mu\text{Ci/g}</math></u>	<u>C=A/B normalization constant</u>
$^{54}\text{Fe}(n,p)^{54}\text{Mn}$	454	668	0.68
$^{58}\text{Ni}(n,p)^{58}\text{Co}$	1056	1540	0.69
$^{238}\text{U}(n,f)^{137}\text{Cs}$	1.21	1.50	0.81
$^{237}\text{Np}(n,f)^{137}\text{Cs}$	6.89	9.12	0.76
$^{238}\text{U}(n,f)^{106}\text{Ru}$	10.3	15.1	0.68
$^{237}\text{Np}(n,f)^{106}\text{Ru}$	49.3	62.8	0.78

(a) Average of four dosimeter wires from Table D-2.

(b) Average of four dosimeter locations in calculational model.

Table 6-3. Normalized Flux Spectra, Flux per MeV for Range ( $E > \text{MeV}$ )

Energy range, MeV	At center of Capsule	T/4 in pressure vessel	$^{235}\text{U}$ fission
12.2-15.0	0.0003	0.0005	0.0002
10.0-12.2	0.0016	0.0024	0.0009
8.18-10.0	0.0057	0.0079	0.0035
6.36-8.18	0.0158	0.0196	0.0126
4.96-6.36	0.0391	0.0441	0.0369
4.06-4.96	0.0594	0.0610	0.0775
3.01-4.06	0.0857	0.0786	0.145
2.46-3.01	0.185	0.169	0.232
2.35-2.46	0.307	0.279	0.279
1.83-2.35	0.312	0.296	0.331
1.11-1.83	0.529	0.517	0.444
1.0 -1.11	0.729	0.856	0.412

(a) Used to evaluate reaction cross sections (1/E tail added to lower energy groups).

Table 6-4. Neutron Fluence

	$E > 1 \text{ MeV}$		$E > 0.1 \text{ MeV}$	
	Fast flux, $\text{n/cm}^2\text{-s}$	Fast fluence for cycle 1A (268.8 EFPD)	Flux, $\text{n/cm}^2\text{-s}$	Fluence for cycle 1A (268.8 EFPD)
Capsule center	4.51(+10)	1.05(+18)	1.02(+11)	2.37(+18)
Pressure vessel wall (max)	1.22(+10)	2.83(+17)	2.51(+10)	5.83(+17)

Table 6-5. Predicted Fast Fluence in Pressure Vessel at Maximum Location<sup>(a)</sup>

Cycle	Power, MWt	EFPY		Vessel flux, n/cm <sup>2</sup> -s	Fluence, n/cm <sup>2</sup>	
		Interval	Total		Interval	Total <sup>(b)</sup>
1A	2452	0.74	0.74	1.2(+10)	2.8(+17)	2.8(+17)
1B	2452	0.47	1.21	1.5(+10)	2.2(+17)	5.0(+17)
2	2452	0.46	1.67	1.7(+10)	2.5(+17)	7.5(+17)
3	2452	0.88	2.55	1.44(+10)	4.0(+17)	1.2(+18)
4	2544	0.94	3.49	1.29(+10)	3.8(+17)	1.6(+18)
5	2544	1.09	4.58	1.24(+10)	4.3(+17)	2.0(+18)
>5	2544	3.42	8.0	1.24(+10)	1.4(+18)	3.4(+18)
>5	2544	24.0	32.0	1.24(+10)	9.4(+18)	1.3(+19)

(a) Inside surface of the base metal at an azimuthal location about 7 to 11° from a major core axis and an elevation near the core midplane.

(b) Maximum fluence can be translated to T/4, 3T/4, and outer surface locations with the factors 1/1.8, 1/7.7, and 1/21, respectively.

Table 6-6. Calculated Neutron Fluence for Material Specimens (n/cm<sup>2</sup>)Tensile Specimens

Weld metal	$1.0 \times 10^{18}$
Base metal	$1.0 \times 10^{18}$

Charpy Specimens

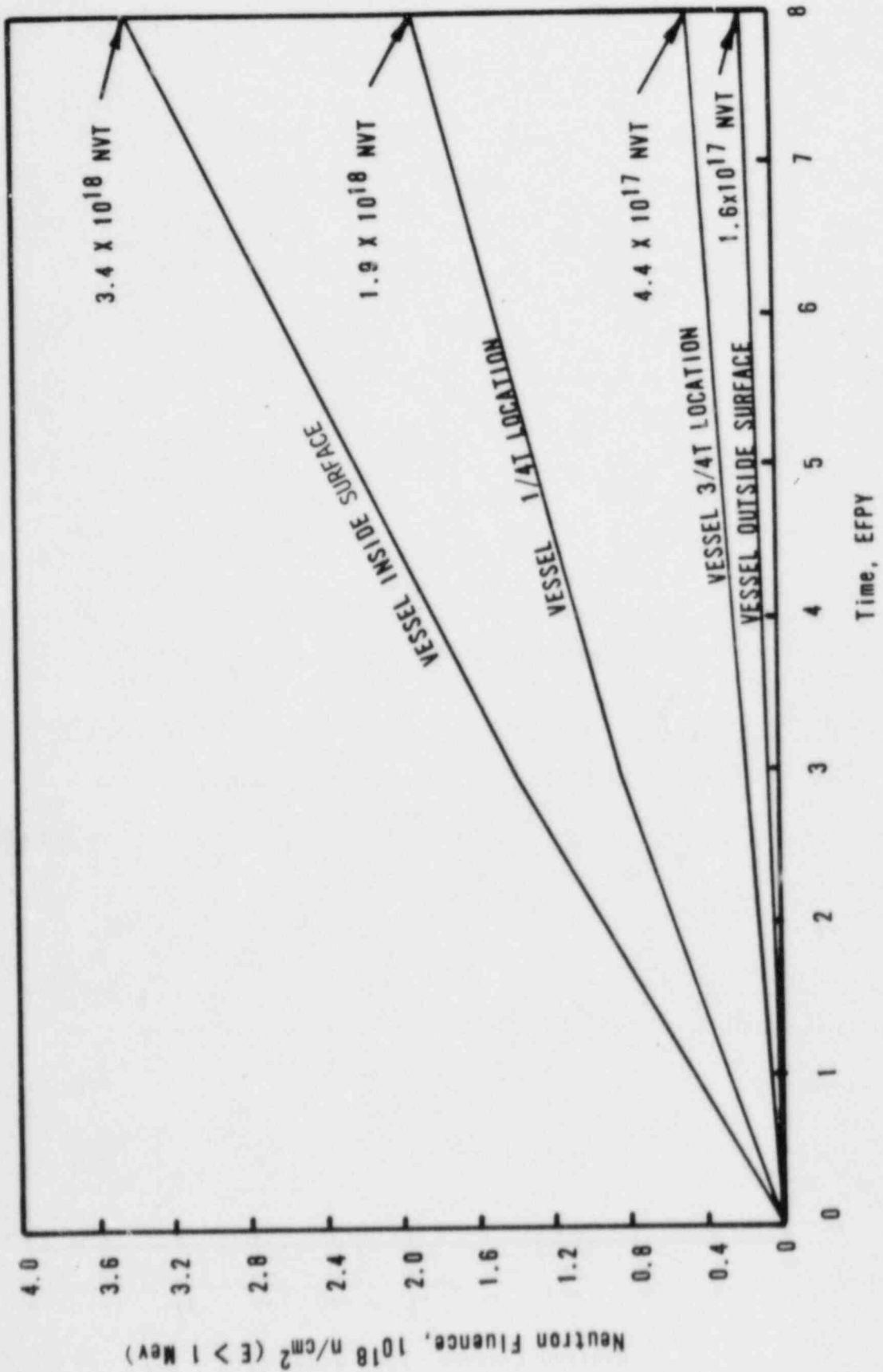
Weld metal	$1.17 \times 10^{18}$
Base metal	$1.0 \times 10^{18}$
Heat-affected zone	$8.4 \times 10^{17}$

Compact Fracture Specimens

Weld metal	$1.0 \times 10^{18}$
------------	----------------------



Figure 6-1. Predicted Fast Neutron Fluences at Various Locations Through Reactor Vessel Wall for First 8 EFPY



## 7. DISCUSSION OF CAPSULE RESULTS

### 7.1. Preirradiation Property Data

A review of the unirradiated properties of the reactor vessel core belt region indicated no significant deviation from expected properties except in the case of the upper shelf properties of the weld metal. Based on the predicted end-of-service peak neutron fluence value at the 1/4T vessel wall location and the copper content of this weld, it is predicted that the end-of-service Charpy upper shelf energy (USE) will be below 50 ft-lb. This weld was selected for inclusion in the surveillance program in accordance with the criteria in effect at the time the program was designed for Crystal River Unit 3. The applicable selection criterion was based on the unirradiated properties only.

### 7.2. Irradiated Property Data

#### 7.2.1. Tensile Properties

Table 7-1 compares irradiated and unirradiated tensile properties. At both room temperature and elevated temperature, the ultimate and yield strength changes in the base metal as a result of irradiation and the corresponding changes in ductility are negligible. There appears to be some strengthening, as indicated by increases in ultimate and yield strength and similar decreases in ductility properties. All changes observed in the base metal are such as to be considered within acceptable limits. The changes at both room temperature and 580F in the properties of the base metal are greater than those observed for the weld metal, indicating a greater sensitivity of the base metal to irradiation damage. In either case, the changes in tensile properties are insignificant relative to the analysis of the reactor vessel materials at this period in service life.

#### 7.2.2. Impact Properties

The behavior of the Charpy V-notch impact data is more significant to the calculation of the reactor system's operating limitations. Table 7-2 compares

the observed changes in irradiated Charpy impact properties with the predicted changes as shown in Figures 7-1 through 7-3.

The 50-ft-lb transition temperature shift for the base metal was in good agreement with the shift that would be predicted according to Regulatory Guide 1.99. The less-than-ideal comparison may be attributed to the spread in the data of the unirradiated material combined with a minimum of data points to establish the irradiated curve. Under these conditions, the comparison indicates that the estimating curves in RG 1.99 for medium-copper materials and at low fluence levels are reasonably accurate for predicting the 50-ft-lb transition temperature shifts.

The 30-ft-lb transition temperature shift for the base metal is not in as good agreement with the value predicted according to Regulatory Guide 1.99, although it would be expected that these values would exhibit better comparison when it is considered that a major portion of the data used to develop Regulatory Guide 1.99 was taken at the 30-ft-lb temperature.

The increase in the 35-mil lateral expansion transition temperature is compared with the shift in  $RT_{NDT}$  curve data in a manner similar to the comparison made for the 50-ft-lb transition temperature shift. These data show a behavior similar to that observed from the comparison of the observed and predicted 50-ft-lb transition data.

All the transition temperature measurements for the weld metal are in poor agreement with the predicted shift. This can be attributed to the chemistry of the weld metal as compared to the nominal chemistry of normal weld metal for which the prediction curves were developed. The abnormal silicon content and low nickel content combine to make the weld metal less sensitive than the base metal. This being the case, it would not be expected that the current prediction techniques will apply to the weld metal.

The data for the decrease in Charpy USE with irradiation showed a poor agreement with predicted values for both the base metal and the weld metal. However, the poor comparison of the measured data with the predicted value is not unexpected in view of the lack of data for medium- to high-copper-content materials at low to medium fluence values that were used to develop the estimating curves.

Results from other capsules indicate that the  $RT_{NDT}$  estimating curves have greater inaccuracies at the very low neutron fluence levels ( $\leq 1 \times 10^{18}$  n/cm<sup>2</sup>). This inaccuracy is attributed to the limited data at the low fluence values and of the fact that the majority of the data used to define the curves in RG 1.99 are based on the shift at 30 ft-lb as compared to the current requirement of 50-ft-lb. For most materials the shifts measured at 50 ft-lb/35 MLE are expected to be higher than those measured at 30 ft-lb. The significance of the shifts at 50 ft-lb and/or 35 MLE is not well understood at present, especially for materials having USEs that approach the 50 ft-lb level and/or the 35 MLE level. Materials with this characteristic may have to be evaluated at transition energy levels lower than 50 ft-lb.

The design curves for predicting the shift at 50 ft-lb/35 MLE will probably be modified as data become available; until that time, the design curves for predicting the  $RT_{NDT}$  shift as given in Regulatory Guide 1.99 are considered adequate for predicting the  $RT_{NDT}$  shift of those materials for which data are not available and will continue to be used to establish the pressure-temperature operational limitations for the irradiated portions of the reactor vessel.

The lack of good agreement of the change in Charpy USE is further support of the inaccuracy of the prediction curves at the lower fluence levels. Although the prediction curves are conservative in that they predict a larger drop in upper shelf than is observed for a given fluence and copper content, the conservatism can unduly restrict the operational limitations. These data support the contention that the USE drop curves will have to be modified as more reliable data become available; until that time the design curves used to predict the decrease in USE are conservative.

In evaluating the Charpy data from the CR3-B capsule it is important to note that the weld metal from which the Charpy specimens were fabricated has been identified as "atypical" as described in BAW-10144A<sup>5</sup>. In accordance with the NRC review of BAW-10144A the behavior of the weld metal in Crystal River 3 RVMSP will be monitored to ensure the correct predictive methodology for those weldments that could have been fabricated with "atypical" weld wire. The data from the CR3-B capsule indicate that the atypical weld metal is significantly less sensitive to neutron radiation damage than normal weld metal of the same type.

Table 7-1. Comparison of Tensile Test Results

	<u>Room temp test</u>		<u>Elevated temp test (580F)</u>	
	<u>Unirr</u>	<u>Irrad</u>	<u>Unirr</u>	<u>Irrad</u>
	<u>Base Metal - 4344-1 Transverse</u>			
Fluence, $10^{18}$ n/cm <sup>2</sup> (> 1 MeV)	0	1.0	0	1.0
Ult. tensile strength, ksi	92.2	100.1	90.6	95.6
0.2% yield strength, ksi	69.3	78.1	63.9	69.4
Elongation, %	24	27	23	21
RA, %	62	61	56	49
<u>Weld Metal - WF-209-1<sup>(a)</sup></u>				
Fluence, $10^{18}$ n/cm <sup>2</sup> (> 1 MeV)	0	1.0	0	1.0
Ult. tensile strength, ksi	93.8	98.7	88.5	90.6
0.2% yield strength, ksi	77.0	83.1	67.5	69.3
Elongation, %	29	27	20	25
RA, %	62	62	48	53

(a) Atypical weld metal.

Table 7-2. Observed Vs Predicted Changes in Irradiated Charpy Impact Properties

<u>Material</u>	<u>Observed</u>	<u>Predicted</u> <sup>(a)</sup>	
<u>Increase in 30-ft-lb trans temp, F</u>			
Base material (C-4344-1)			
Transverse	21	57	
Heat-affected zone (C-4344-1)	70	57	
Weld metal (WF-209-1) <sup>(c)</sup>	28	105	1
<u>Increase in 50-ft-lb trans temp, F</u>			
Base material (C-4344-1)			
Transverse	51	57	
Heat-affected zone (C-4344-1)	64	57	
Weld metal (WF-209-1) <sup>(c)</sup>	13	105	1
<u>Increase in 35-MLE trans temp, F</u>			
Base material (C-4344-1)			
Transverse	35	57 <sup>(b)</sup>	
Heat-affected zone (C-4344-1)	74	57 <sup>(b)</sup>	
Weld metal (WF-209-1) <sup>(c)</sup>	34	105 <sup>(b)</sup>	1
<u>Decrease in Charpy USE, ft-lb</u>			
Base material (C-4344-1)			
Transverse	5	16	
Heat-affected zone (C-4344-1)	5	14	
Weld metal (WF-209-1) <sup>(c)</sup>	9	24	1

(a) These values predicted per Regulatory Guide 1.99, Revision 1.

(b) Based on the assumption that MLE as well as 50 ft-lb transition temperature is used to control the shift in  $RT_{NDT}$ .

(c) Atypical weld metal.

Figure 7-1. Irradiated Vs Unirradiated Charpy Impact Properties of Base Metal

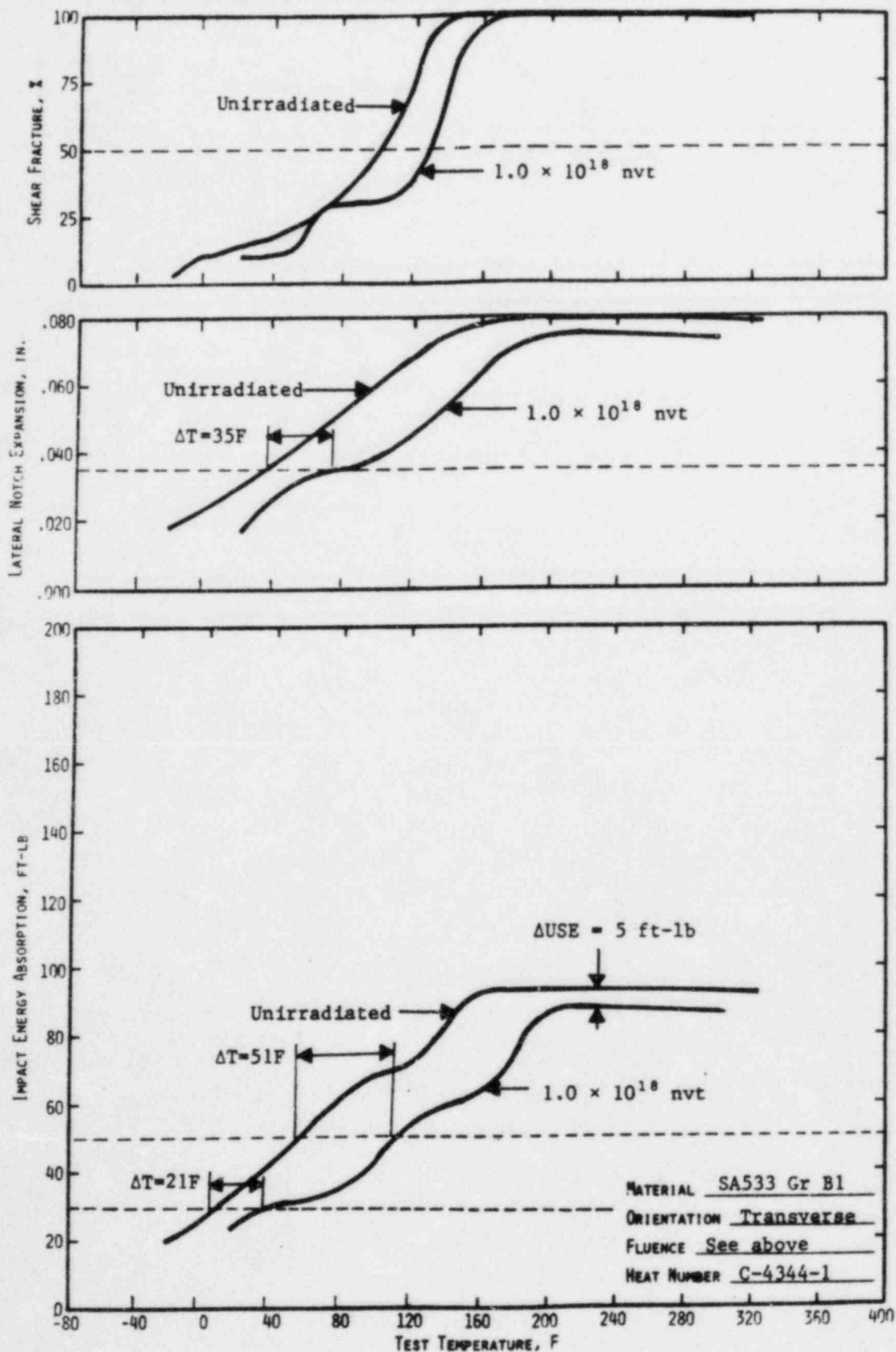


Figure 7-2. Irradiated Vs Unirradiated Charpy Impact Properties of Heat-Affected Zone Material

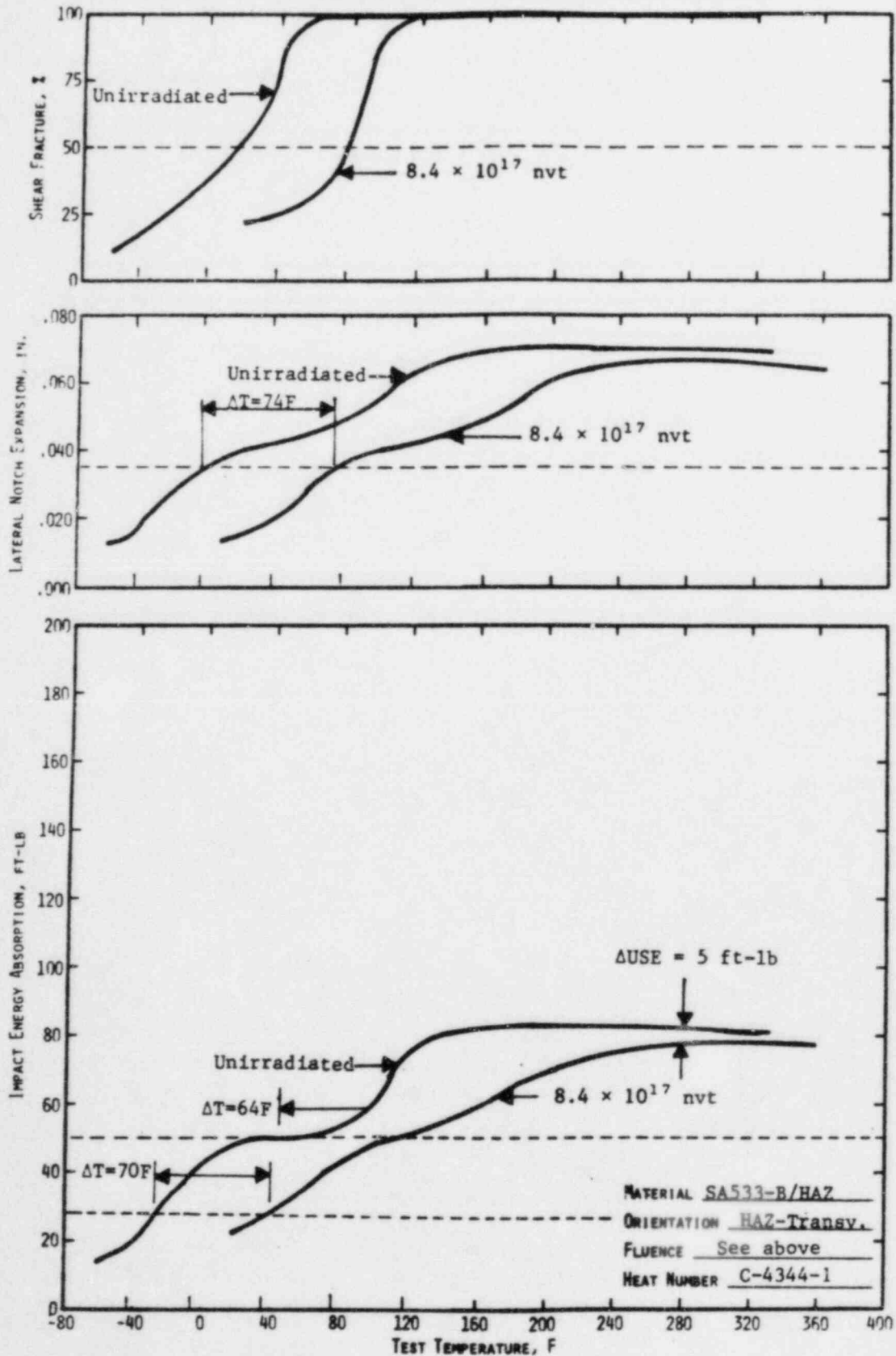
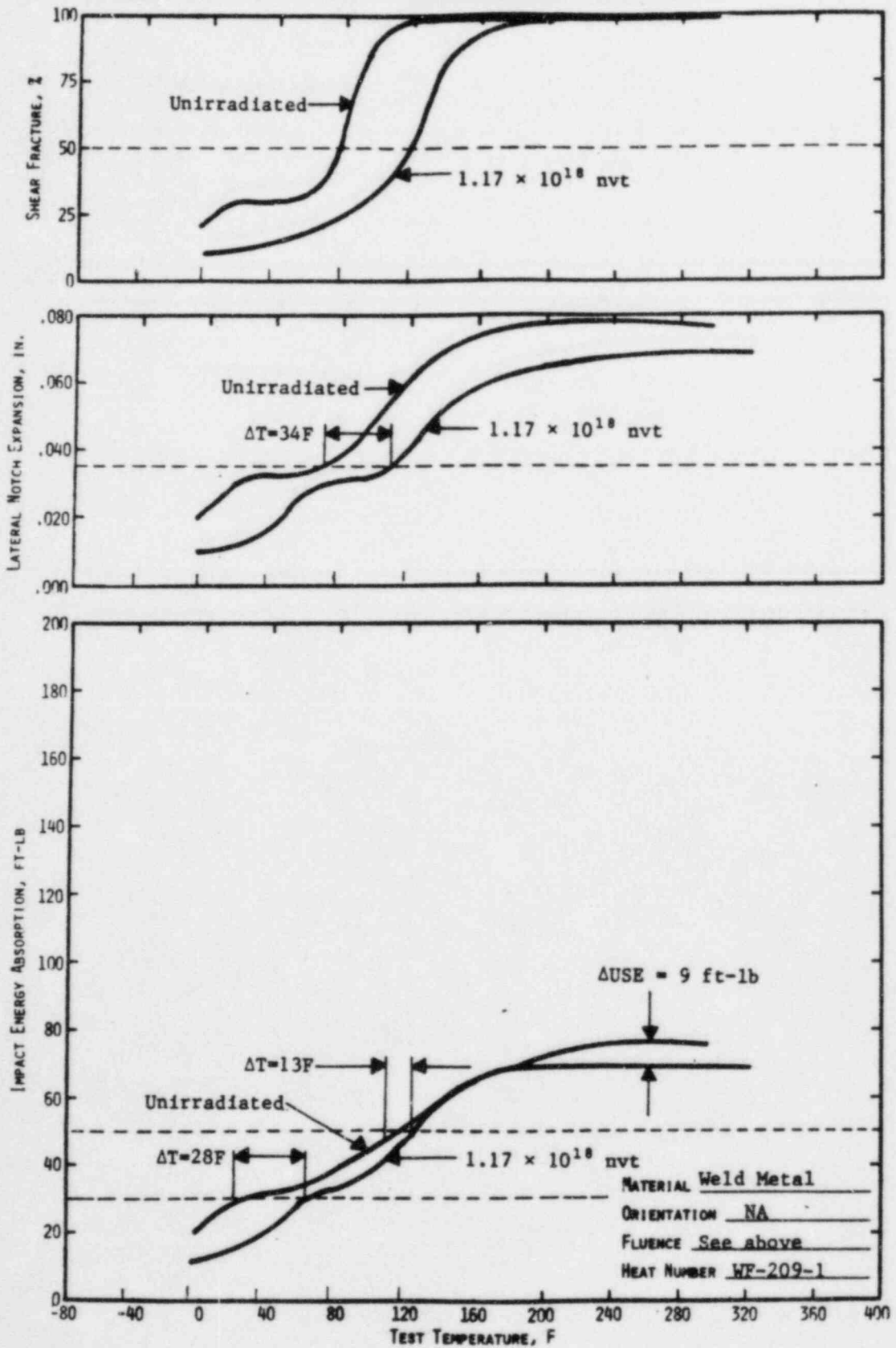




Figure 7-3. Irradiated Vs Unirradiated Charpy Impact Properties of Weld Metal



01325



## 8. DETERMINATION OF RCPB PRESSURE-TEMPERATURE LIMITS

The pressure-temperature limits of the reactor coolant pressure boundary (RCPB) of Crystal River 3 are established in accordance with the requirements of 10 CFR 50, Appendix G. The methods and criteria employed to establish operating pressure and temperature limits are described in topical report BAW-10046.<sup>5</sup> The objective of these limits is to prevent nonductile failure during any normal operating condition, including anticipated operation occurrences and system hydrostatic tests. The loading conditions of interest include the following:

1. Normal operations, including heatup and cooldown.
2. Inservice leak and hydrostatic tests.
3. Reactor core operation.

The major components of the RCPB have been analyzed in accordance with 10 CFR 50, Appendix G. The closure head region, the reactor vessel outlet nozzle, and the beltline region have been identified as the only regions of the reactor vessel, and consequently of the RCPB, that regulate the pressure-temperature limits. Since the closure head region is significantly stressed at relatively low temperatures (due to mechanical loads resulting from bolt preload), this region largely controls the pressure-temperature limits of the first several service periods. The reactor vessel outlet nozzle also affects the pressure-temperature limit curves of the first several service periods. This is due to the high local stresses at the inside corner of the nozzle, which can be two to three times the membrane stresses of the shell. After the first several years of neutron radiation exposure, the  $RT_{NDT}$  of the beltline region materials will be high enough that the beltline region of the reactor vessel will start to control the pressure-temperature limits of the RCPB. For the service period for which the limit curves are established, the maximum allowable pressure as a function of fluid temperature is obtained through a point-by-point comparison of the limits imposed by the closure head region, the outlet nozzle, and the beltline region. The maximum allowable pressure is taken to be the lowest of three calculated pressures.

The limit curves for Crystal River 3 are based on the predicted values of the adjusted reference temperatures of all the beltline region materials at the end of the eighth full-power year. The eighth full-power year was selected because it is estimated that the second surveillance capsule will be withdrawn at the end of the refueling cycle when the estimated fluence corresponds to approximately the ninth full-power year. The time difference between the withdrawal of the first and second surveillance capsule provides adequate time for re-establishing the operating pressure and temperature limits for the period of operation between the second and third surveillance capsule withdrawals.

The unirradiated impact properties were determined for the surveillance beltline region materials in accordance with 10 CFR 50, Appendixes G and H. For the other beltline region and RCPB materials for which the measured properties are not available, the unirradiated impact properties and residual elements, as originally established for the beltline region materials, are listed in Table A-1. The adjusted reference temperatures are calculated by adding the predicted radiation-induced  $\Delta RT_{NDT}$  and the unirradiated  $RT_{NDT}$ . The predicted  $\Delta RT_{NDT}$  is calculated using the respective neutron fluence and copper and phosphorus contents. Figure 8-1 illustrates the calculated peak neutron fluence at several locations through the reactor vessel beltline region wall and at the center of the surveillance capsules at each of two locations as a function of exposure time. The supporting information for Figure 8-1 is described in BAW-10100.<sup>1</sup> The neutron fluence values of Figure 8-1 are the predicted fluences, which have been demonstrated (section 6) to be conservative. The design curves of Regulatory Guide 1.99\* were used to predict the radiation-induced  $\Delta RT_{NDT}$  values as a function of the material's copper and phosphorus content and neutron fluence.

The neutron fluences and adjusted  $RT_{NDT}$  values of the beltline region materials at the end of the eighth full-power year are listed in Table 8-1. The neutron fluences and adjusted  $RT_{NDT}$  values are given for the 1/4T and 3/4T vessel wall locations (T = wall thickness). The assumed  $RT_{NDT}$  of the closure head region and the outlet nozzle steel forgings is 60F, in accordance with BAW-10046P.<sup>5</sup>

- - - - -  
\*Revision 1, January 1976.

Figure 8-2 shows the reactor vessel's pressure-temperature limit curve for normal heatup. This figure also shows the core criticality limits as required by 10 CFR 50, Appendix G. Figure 8-3 and 8-4 show the vessel's pressure-temperature limit curve for normal cooldown and for heatup during inservice leak and hydrostatic tests, respectively. All pressure-temperature limit curves are applicable up to the ninth effective full-power year. Protection against nonductile failure is ensured by maintaining the coolant pressure below the upper limits of the pressure-temperature limit curves. The acceptable pressure and temperature combinations for reactor vessel operation are below and to the right of the limit curve. The reactor is not permitted to go critical until the pressure-temperature combinations are to the right of the criticality limit curve. To establish the pressure-temperature limits for protection against nonductile failure of the RCPB, the limits presented in Figures 8-2 through 8-4 must be adjusted by the pressure differential between the point of system pressure measurement and the pressure on the reactor vessel controlling the limit curves. This is necessary because the reactor vessel is the most limiting component of the RCPB.

Table 8-1. Data for Preparation of Pressure-Temperature Limit Curves for Crystal River Unit 3, Applicable Through 8 EFPY

Material identifi'n		Beltline region location	Weldment location			Unirr RT, NDT <sup>a</sup> F	Content		Neutron fluence at end of 8 EFPY (E > 1 MeV), n/cm <sup>2</sup>		Radiation-induced ΔRT <sub>NDT</sub> at end of 8 EFPY, ΔF <sup>(b)</sup>		Adjusted RT <sub>NDT</sub> at end of 8 EFPY, F	
Heat No.	Type		Core midplane to weld $\bar{q}$ , cm	Location from major axis, °	Welds at 1/4 T ?		Cu, %	P, %	At 1/4 T	At 3/4 T	At 1/4 T	At 3/4 T	At 1/4 T	At 3/4 T
123V190	SA508, CI 2	Lower nozzle belt	--	--	--	+10	0.05	0.008	1.5E18 <sup>(a)</sup>	3.4E17	16	7	26	17
C-4344-1	SA533B, CI 1	Upper shell	--	--	--	+20	0.20	0.008	1.9E18	4.4E17	70	34	90	54
C-4344-2	SA533B, CI 1	Upper shell	--	--	--	+20	0.20	0.008	1.9E18	4.4E17	70	34	90	54
C-4347-1	SA533B, CI 1	Lower shell	--	--	--	-20	0.12	0.013	1.9E18	4.4E17	46	22	26	2
C-4347-2	SA533B, CI 1	Lower shell	--	--	--	+45	0.12	0.013	1.9E18	4.4E17	46	22	91	67
WF-169	Weld	Upper circ (60%)	+123	--	No	(+20)	(-)	(-)	--	3.4E17	--	33	--	53
SA-1769	Weld	Upper circ (40%)	+123	--	Yes	(+20)	(-)	(-)	1.5E18	--	108	--	128	--
WF-8	Weld	Upper long. (100%)	--	17	Yes	(+20)	(-)	(-)	1.8E18	4.2E17	110	53	130	73
WF-18	Weld	Upper long. (100%)	--	17	Yes	(+20)	(-)	(-)	1.8E18	4.2E17	110	53	130	73
WF-70	Weld	Middle circ (100%)	-6	--	Yes	(+20)	(-)	(-)	1.9E18	4.4E17	157	76	177	96
SA-1580	Weld	Lower long. (100%)	--	20	Yes	(+20)	(-)	(-)	1.6E18	3.7E17	114	55	134	75
WF-154	Weld	Lower circ (100%)	-249	--	Yes	(+20)	(-)	(-)	1.1E16	2.5E15	10	Neg.	30	20
Atypical	Weld	Middle circ (100%)	-6	--	Yes	+90 <sup>(b)</sup>	--	--	1.9E18	4.4E17	46 <sup>(b)</sup>	22 <sup>(b)</sup>	136	112

Note: ( ) = Estimated value per BAW-10046A, Rev. 1, July 1977.<sup>8</sup>  
 (-) = Values per BAW-1511P, October 1980.<sup>7</sup>

(a) Per Regulatory Guide 1.99, Rev. 1.<sup>8</sup>

(b) Per BAW-10144A, February 1980.<sup>5</sup>

8-4

Babcock & Wilcox

Figure 8-1. Fast Neutron Fluence of Surveillance Capsule Center Compared to Various Locations Through Reactor Vessel Wall for First 8 EPY

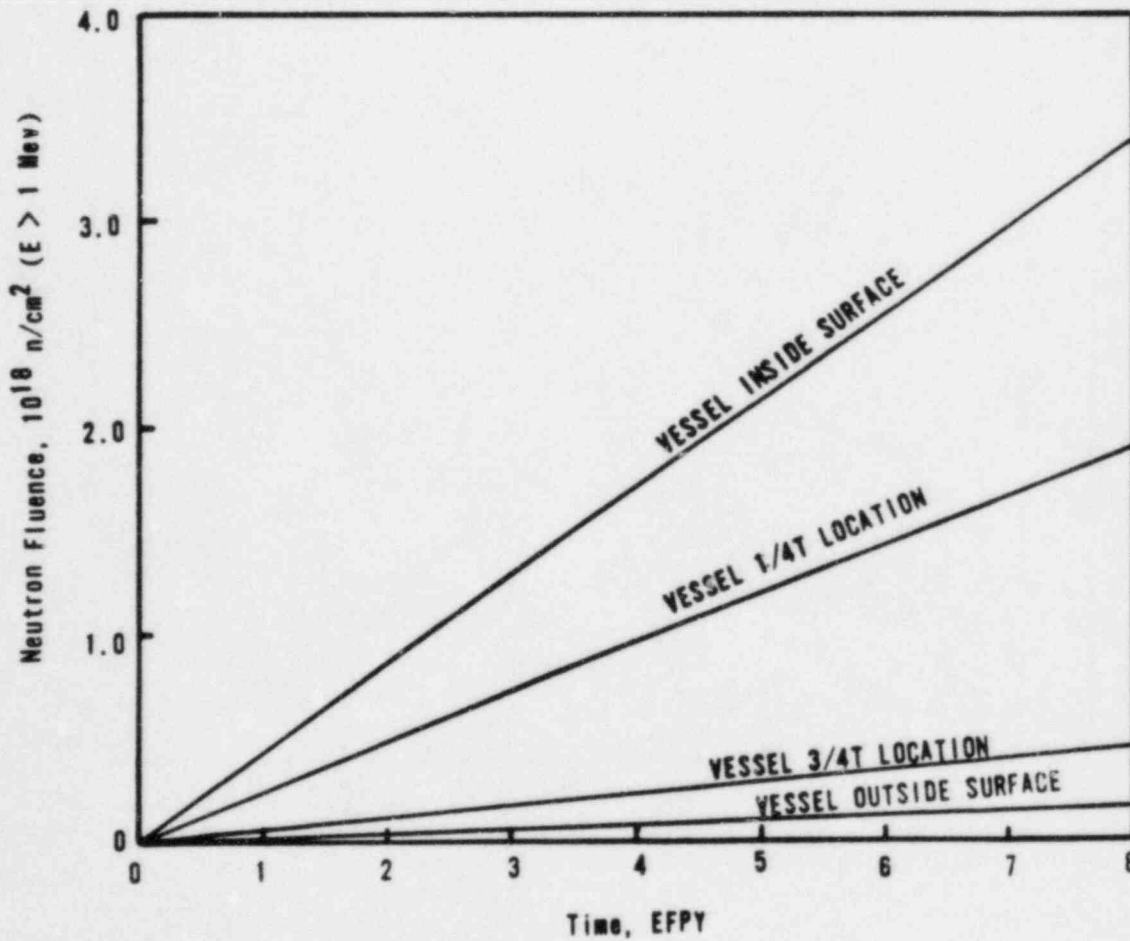
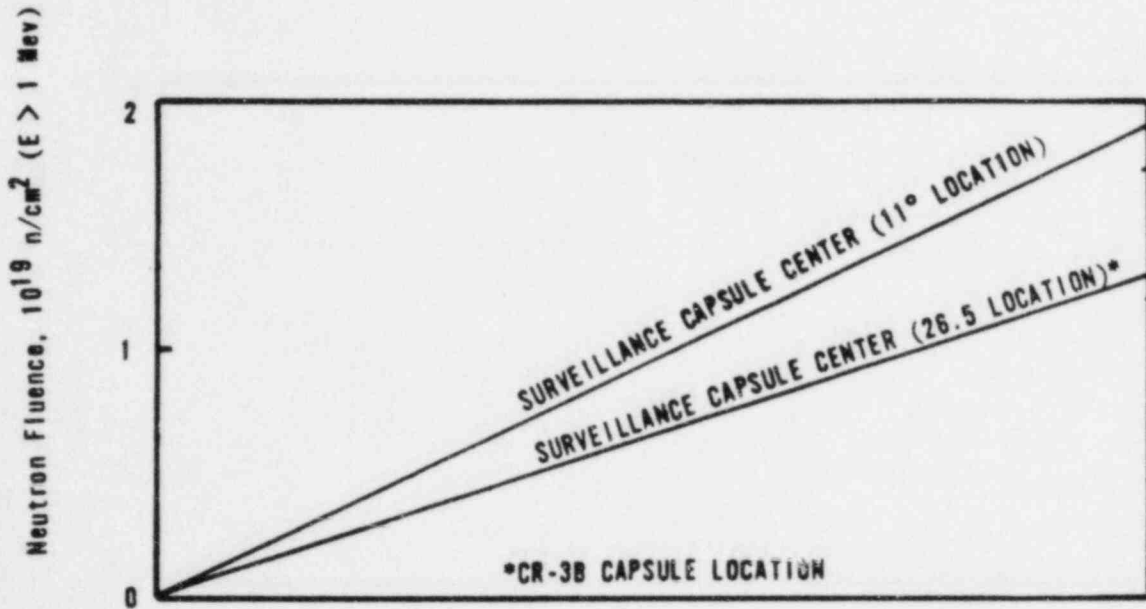


Figure 8-2. Reactor Vessel Pressure-Temperature Limit Curves for Normal Operation - Heatup, Applicable for First 8 EFPPY

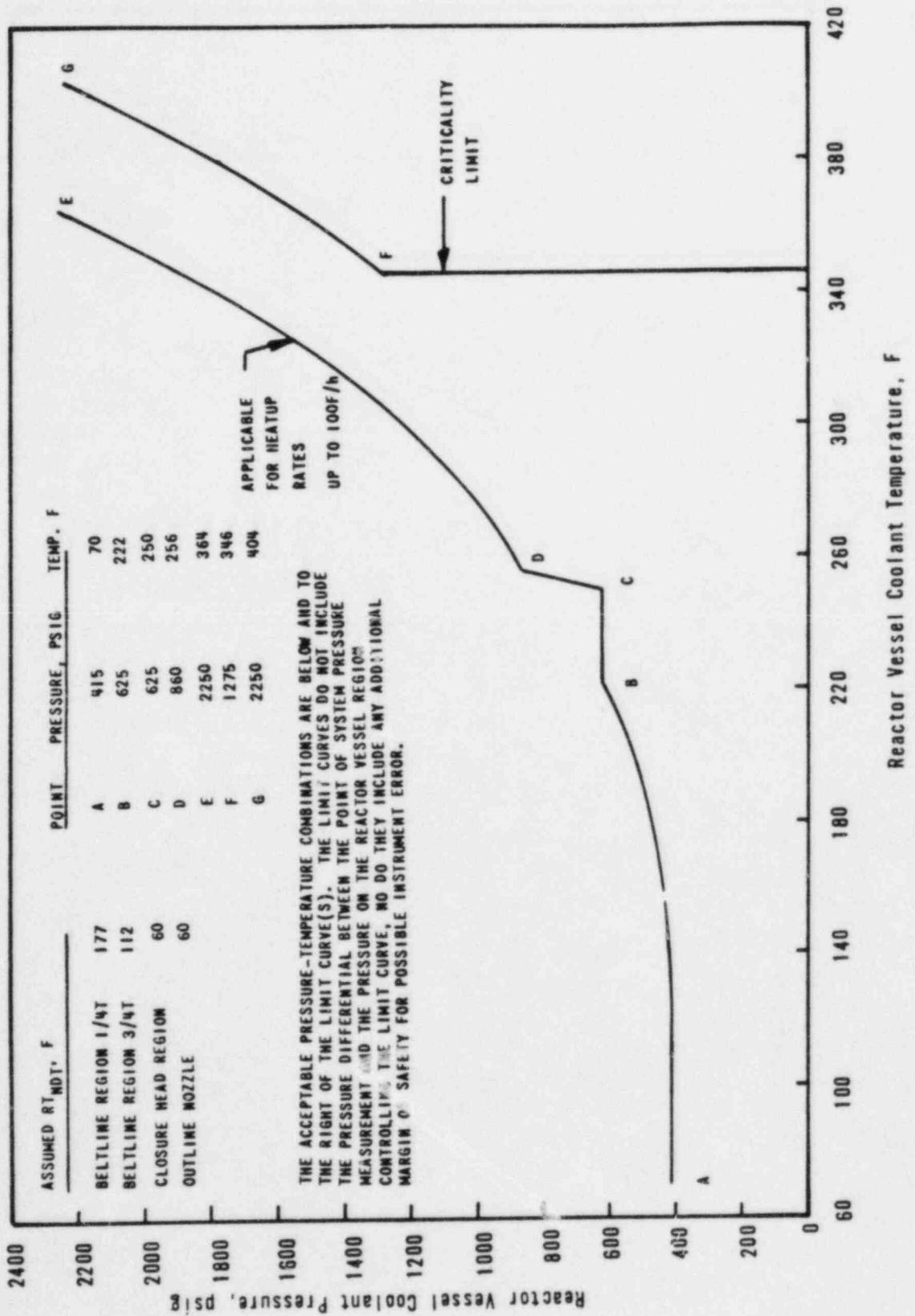


Figure 8-3. Reactor Vessel Pressure-Temperature Limit Curve for Normal Operation - Cooldown Applicable for First 8 EPY

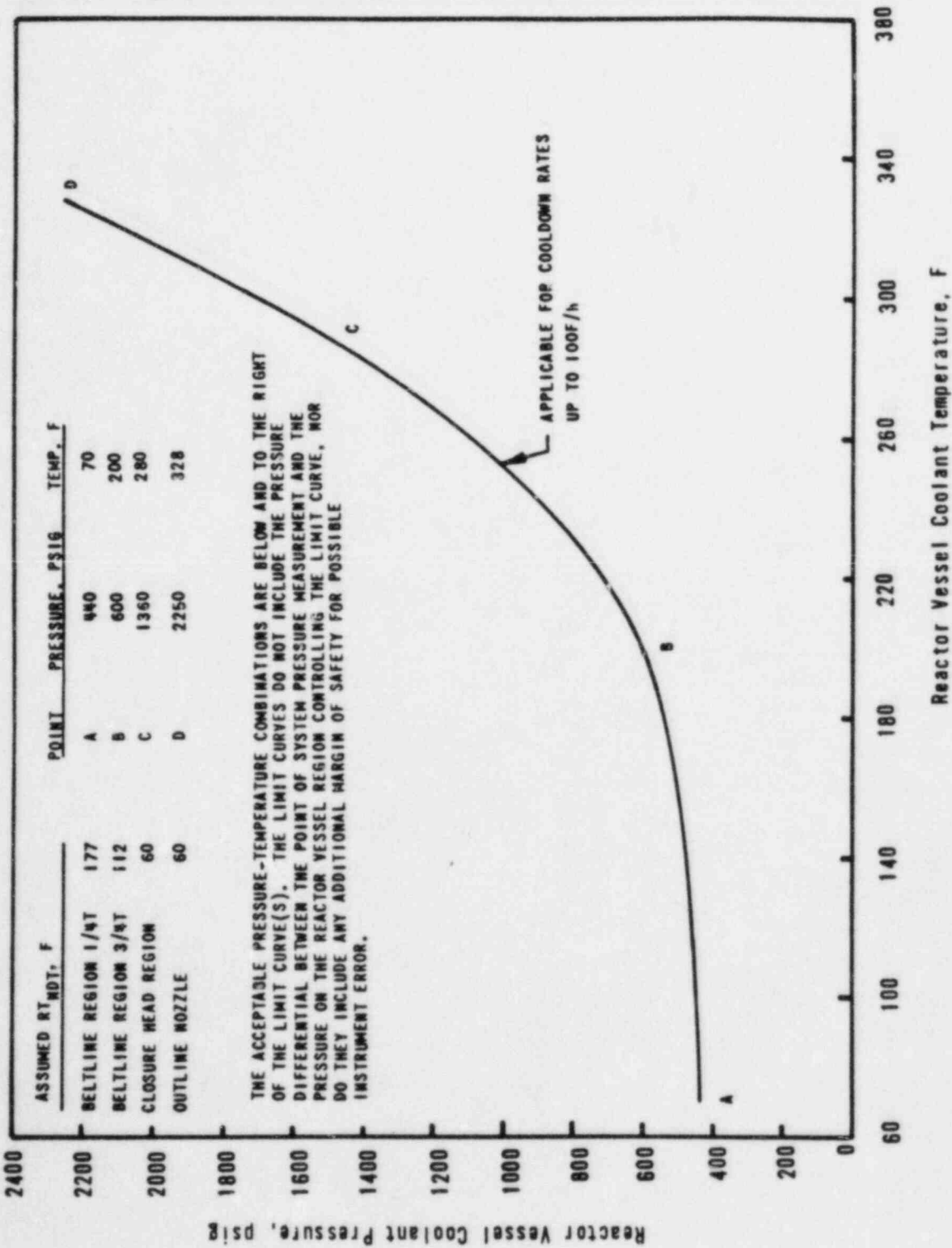
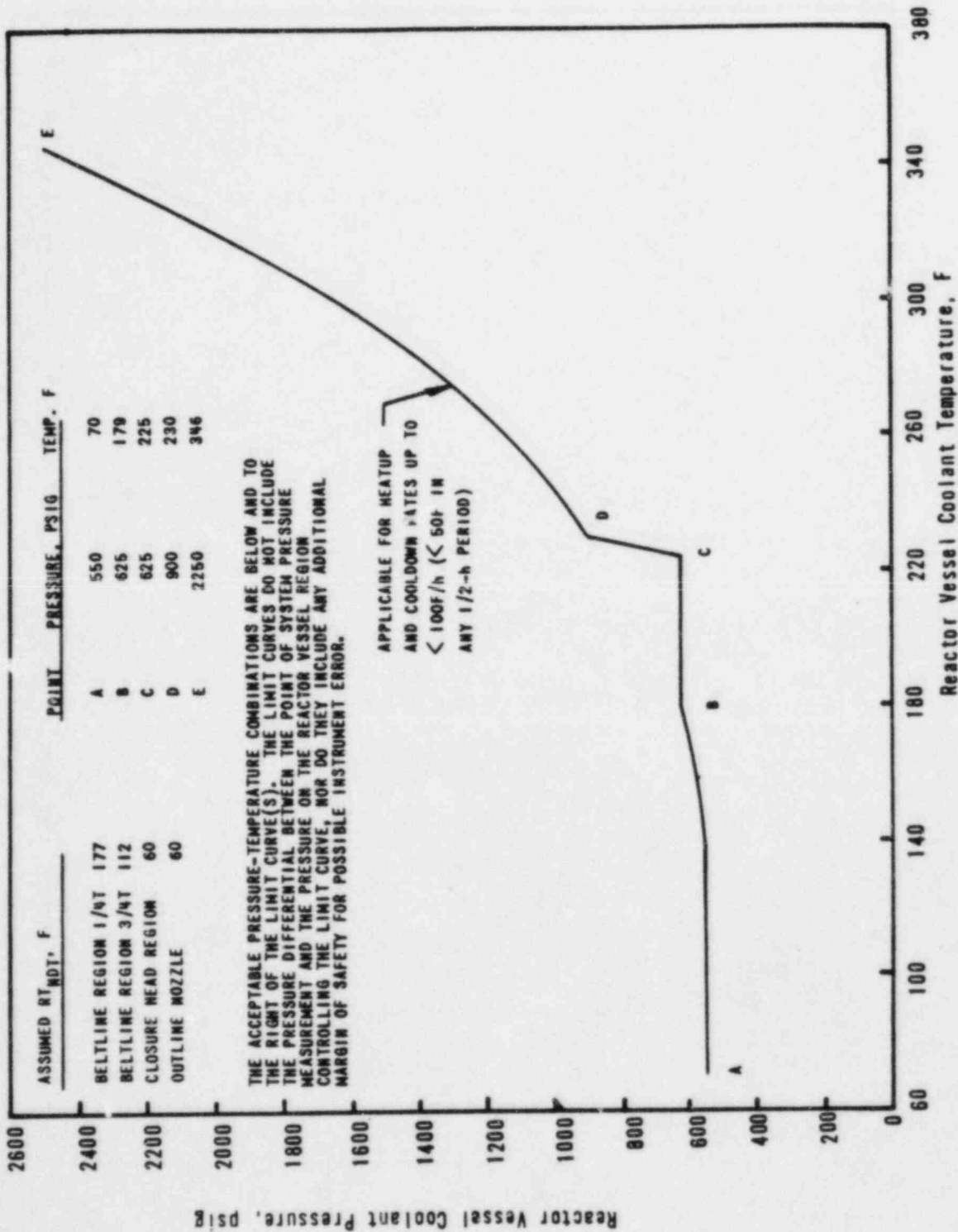




Figure 8-4. Reactor Vessel Pressure-Temperature Limit Curve for Inservice Leak and Hydrostatic Tests, Applicable for First 8 EFPY



## 9. SUMMARY OF RESULTS

The analysis of the reactor vessel material contained in the first surveillance capsule CR3-B removed from the Crystal River Unit 3 pressure vessel led to the following conclusions:

1. The capsule received an average fast fluence of  $1.05 \times 10^{18}$  n/cm<sup>2</sup> (E > 1 MeV). The predicted fast fluence for the reactor vessel T/4 location at the end of the first fuel cycle is  $1.58 \times 10^{17}$  n/cm<sup>2</sup> (E > 1 MeV).
2. The fast fluence of  $1.05 \times 10^{18}$  n/cm<sup>2</sup> (E > 1 MeV) increased the RT<sub>NDT</sub> of the capsule reactor vessel core region shell materials a maximum of 70F.
3. Based on a ratio of 5.4 between the fast flux at the surveillance capsule location to that at the vessel wall and an 80% load factor, the projected fast fluence that the Crystal River Unit 3 reactor pressure vessel will receive in 40 calendar years' operation is  $1.3 \times 10^{19}$  n/cm<sup>2</sup> (E > 1 MeV).
4. The increase in the RT<sub>NDT</sub> for the base plate material was in good agreement with that predicted by the currently used design curves of  $\Delta RT_{NDT}$  versus fluence.
5. The increase in the RT<sub>NDT</sub> for the weld metal was not in good agreement with that predicted by the currently used design curves of  $\Delta RT_{NDT}$  versus fluence because of the difference in chemical composition.
6. The current techniques used for predicting the change in Charpy impact upper shelf properties due to irradiation are conservative.
7. The analysis of the neutron dosimeters demonstrated that the analytical techniques used to predict the neutron flux and fluence were accurate.
8. The thermal monitors indicated that the capsule design was satisfactory for maintaining the specimens within the desired temperature range.

## 10. SURVEILLANCE CAPSULE REMOVAL SCHEDULE

Based on the post-irradiation test results of capsule CR3-B, the following schedule is recommended for examination of the remaining capsules in the Crystal River Unit 3 reactor vessel surveillance program:

Capsule ID	Evaluation schedule <sup>(a)</sup>			Est. date data available <sup>(b)</sup>	
	Est. capsule fluence, $10^{19}$ n/cm <sup>2</sup>	Est. fluence, $10^{19}$ n/cm <sup>2</sup>			
		Surface	1/4 T		
CR3-A	Standby	--	--	--	<i>Cycle</i>
CR3-C	0.7	0.13	0.07	<i>S<sub>p</sub></i> 1983	<i>4</i>
CR3-D <sup>(c)</sup>	1.1	0.21	0.11	<i>S<sub>p</sub></i> 1986	<i>6</i>
CR3-E	1.7	0.32	0.18	<i>S<sub>p</sub></i> 1989	<i>9</i>
CR3-F <sup>(c)</sup>	3.0	0.56	0.31	1994	<i>11</i>

(a) In accordance with BAW-10100A and E-185-79.

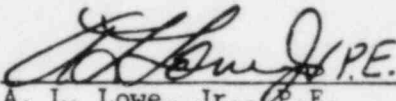
(b) Estimated date based on 0.8 plant operation factor.

(c) Capsules contain weld metal compact fracture specimens.

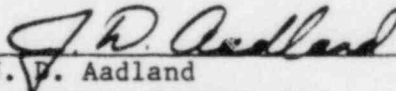
*Revised 1/8*

11. CERTIFICATION

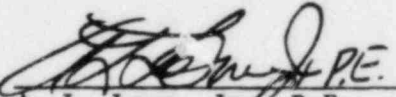
The specimens were tested, and the data obtained from Crystal River Unit 3 surveillance capsule CR3-B were evaluated using accepted techniques and established standard methods and procedures in accordance with the requirements of 10 CFR 50, Appendixes G and H.

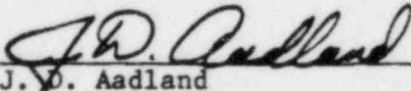
 P.E. 30 June 1981  
A. L. Lowe, Jr., P.E. Date  
Project Technical Manager

This report has been reviewed for technical content and accuracy.

 7/10/81  
J. P. Aadland Date  
Component Engineering

Certification, Revision 1

 P.E. 17 June 1982  
A. L. Lowe, Jr., P.E. Date  
Project Technical Manager

 6/17/82  
J. P. Aadland Date  
Component Engineering

## 12. REFERENCES

- <sup>1</sup> H. S. Palme, G. S. Carter, and C. L. Whitmarsh, Reactor Vessel Material Surveillance Program - Compliance With 10 CFR 50 Appendix H, for Oconee-Class Reactors, BAW-10100A, Babcock & Wilcox, Lynchburg, Virginia, February 1975.
- <sup>2</sup> DOT 3.5 - Two-Dimensional Discrete Ordinates Radiation Transport Code, CCC-276, WANL-TME-1982, Oak Ridge National Laboratory, December 1969.
- <sup>3</sup> CASK - 40-Group Coupled Neutron and Gamma-Ray Cross Section Data, RSIC-DLC-23, Radiation Shielding Information Center.
- <sup>4</sup> C. L. Whitmarsh, Pressure Vessel Fluence Analysis for 177-FA Reactors, BAW-1485, June 1978.
- <sup>5</sup> K. E. Moore, et al., Evaluation of the Atypical Weldment, BAW-10144A, Babcock & Wilcox, Lynchburg, Virginia, February 1980.
- <sup>6</sup> H. S. Palme, et al., Methods of Compliance With Fracture Toughness and Operational Requirements of 10 CFR 50, Appendix G, BAW-10046A, Rev. 1, Babcock & Wilcox, Lynchburg, Virginia, July 1977.
- <sup>7</sup> A. L. Lowe, Jr., et al., Irradiation-Induced Reduction in Charpy Upper Shelf Energy of Reactor Vessel Welds, BAW-1511P, Babcock & Wilcox, Lynchburg, Virginia, October 1980.
- <sup>8</sup> Regulatory Guide 1.99, Revision 1, "Effects of Residual Elements on Predicted Radiation Damage to Reactor Vessel Materials," U.S. Nuclear Regulatory Commission, Washington, D.C., April 1977.

APPENDIX A

Reactor Vessel Surveillance Program --  
Background Data and Information

### 1. Material Selection Data

The data used to select the materials for the specimens in the surveillance program, in accordance with E-185-73, are shown in Table A-1. The locations of these materials within the reactor vessel are shown in Figures A-1 and A-2.

### 2. Definition of Beltline Region

The beltline region of Crystal River Unit 3 was defined in accordance with the data given in BAW-10100A.

### 3. Capsule Identification

The capsules used in the Crystal River Unit 3 surveillance program are identified below by identification number, type, and location.

#### Capsule Cross Reference Data

<u>Number</u>	<u>Type</u>	<u>Location</u>
CR3-A	A	Upper
CR3-B	B	Lower
CR3-C	A	Upper
CR3-D	B	Lower
CR3-E	A	Upper
CR3-F	B	Lower

### 4. Specimens per Surveillance Capsule

See Tables A-2, A-3 and A-4.

Table A-1. Unirradiated Impact Properties and Residual Element Content Data of Beltline Region Materials Used for Selection of Surveillance Program Materials - Crystal River Unit 3

Material ident. heat No.	Material type	Beltline region location	Distance, core midplane to weld centerline, cm	Drop wt. T <sub>NDT</sub> F	Charpy data, CVN				RT NDT* F	Chemistry, %			
					Longitudinal At 10F ft-lb	Transverse				Cu	P	S	Ni
						50 ft-lb, F	35 MLE, F	USE, ft-lb					
ARM96	SA-508, C1 2	Nozzle belt	--	20	11,12,13	--	--	--	10	0.054	0.008	0.006	--
C-4344-1	SA-533, Gr B	Upper shell	--	-10	39(F), 32, 32	80	--	88	20	0.20	0.008	0.016	--
C-4344-2	SA-533, Gr B	Upper shell	--	-10	20(F), 33	80	--	88	20	0.20	0.008	0.016	--
C-4347-1	SA-533, Gr B	Lower shell	--	-20	42, 36, 61	--	--	--	-20	0.12	0.013	0.015	--
C-4347-2	SA-533, Gr B	Lower shell	--	-20	9, 9, 24	100	--	119	40	0.12	0.013	0.015	--
WF-8	Weld	Upper long. seam (100%)	--	--	45, 38, 30	--	--	--	--	0.20	0.009	0.009	--
WF-18	Weld	Upper long. seam (100%)	--	--	45, 46, 38	--	--	--	--	0.105	0.019	0.004	--
WF-169	Weld	Upper circ seam (60% OD)	123	--	36, 43, 42	--	--	--	--	0.106	0.014	0.013	--
SA-1769	Weld	Upper circ seam (40% ID)	123	--	36, 35, 38	--	--	--	--	0.19	0.021	0.016	--
WF-70	Weld	Middle circ seam (100%)	-62	--	39, 35, 44	--	--	--	--	0.27	0.014	0.011	--
SA-1580	Weld	Lower long. seam (100%)	--	--	49, 41, 40	--	--	--	--	0.22	0.015	0.013	--
WF-154	Weld	Lower long. seam (100%)	--	--	41, 37, 43	--	--	--	--	0.20	0.015	0.021	--
WF-209-1	Weld	Surveillance	--	-50	29, 30, 32	103	--	63	43	0.30	0.020	0.005	--

A-3



Table A-2. Test Specimens for Determining Material Baseline Properties

<u>Material description</u>	<u>No. of test specimens</u>			
	<u>Tension</u>		<u>CVN impact</u>	<u>Compact-tension</u> <sup>(b)</sup>
	<u>70F</u>	<u>600F</u> <sup>(a)</sup>		
<u>Heat NN</u>				
Base metal				
Transverse direction	3	3	15	--
Longitudinal direction	3	3	15	--
Heat-affected zone (HAZ)				
Transverse direction	3	3	15	--
Longitudinal direction	<u>3</u>	<u>3</u>	<u>15</u>	<u>--</u>
Total	12	12	60	--
<u>Heat PP</u>				
Base metal				
Transverse direction	3	3	15	--
Longitudinal direction	3	3	15	--
Heat-affected zone (HAZ)				
Transverse direction	3	3	15	--
Longitudinal direction	<u>3</u>	<u>3</u>	<u>15</u>	<u>--</u>
Total	12	12	60	--
Weld metal				
Longitudinal direction	3	3	15	8 1/2 TCT 4 1 TCT

(a) Test temperature to be the same as irradiation temperature.

(b) Test temperature to be determined from shift in impact transition curves after irradiation exposure.

Table A-3. Specimens in Upper Surveillance Capsules  
(Designation A, C, and E)

<u>Material description</u>	<u>No. of test specimens</u>	
	<u>Tension</u>	<u>CVN impact</u>
Weld metal	2	12
Weld, HAZ		
Heat NN, transverse	--	12
Heat PP, transverse	--	6
Base metal		
Heat NN, transverse	2	12
Heat PP, transverse	--	6
Correlation material	<u>--</u>	<u>6</u>
Total per capsule	4	54

Table A-4. Specimens in Lower Surveillance Capsules  
(Designation B, D, and F)

<u>Material description</u>	<u>No. of test specimens</u>		
	<u>Tension</u>	<u>CVN impact</u>	<u>1/2 T compact tension</u> <sup>(a)</sup>
Weld metal	2	12	8
Weld, HAZ			
Heat NN, transverse	--	12	--
Base metal			
Heat NN, transverse	<u>2</u>	<u>12</u>	<u>--</u>
Total per capsule	4	36	8

(a) Compact tension specimens precracked per ASTM E399-72.

Figure A-1. Location and Identification of Materials Used in Fabrication of Crystal River 3 Reactor Pressure Vessel

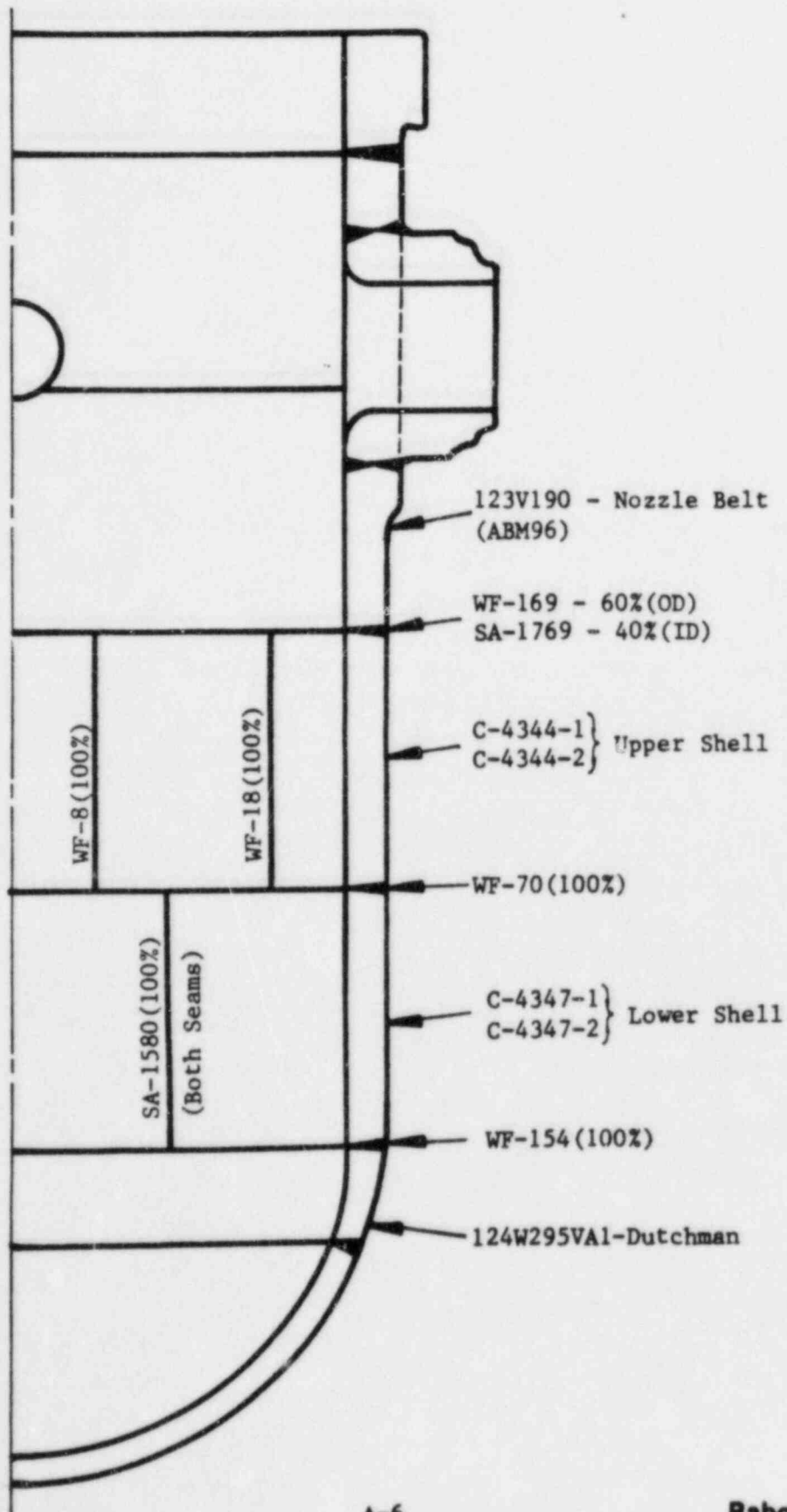


Figure A-2. Location of Longitudinal Welds in Upper and Lower Shell Courses

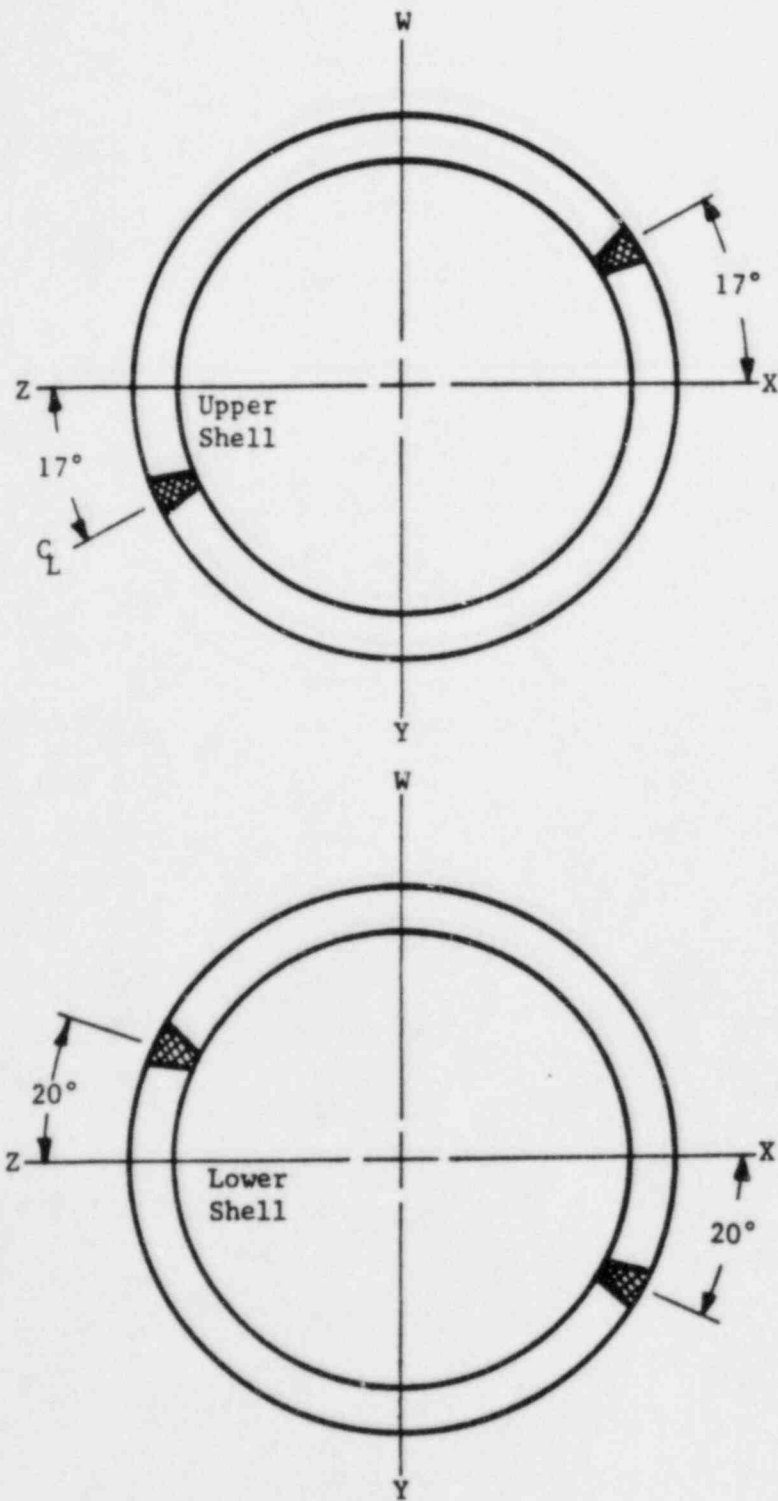
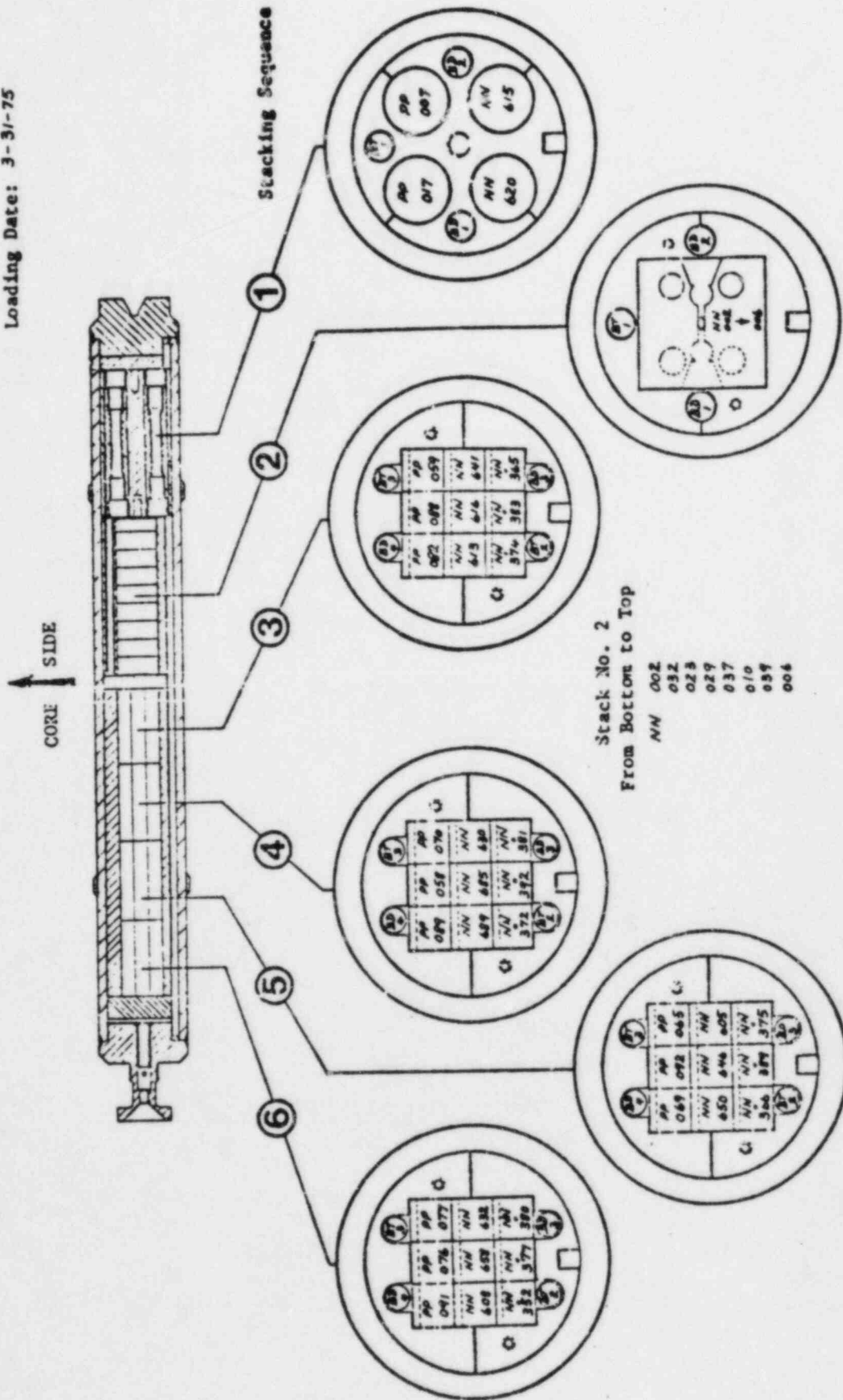


Figure A-3. Loading Diagram for Test Specimens in Lower Surveillance Capsule CR3-B

Contract: MSS 0007

Loading Date: 3-31-75



APPENDIX B  
Preirradiation Tensile Data

Table B-1. Preirradiation Tensile Properties of Shell Plate Material, Heat C-4344-1

Specimen No.	Test temp, F	Strength, psi		Elongation, %		Red'n of area, %
		Yield	Ult.	Unif.	Total	
<u>Longitudinal</u>						
NN-801	RT	70,000	91,875	ES	27	69
NN-802	RT	70,000	91,875	ES	25	69
NN-803	RT	69,375	91,875	11	28	70
Mean	RT	69,790	91,875	11.0	26.6	69.3
Std dev'n		360	0	0	1.5	0.6
NN-804	580	63,750	89,375	14	26	61
NN-805	580	64,375	90,000	12	25	64
NN-806	580	64,375	90,625	11	27	63
Mean	580	64,160	90,000	12.3	26	62.6
Std dev'n		360	625	1.5	1.0	1.5
<u>Transverse</u>						
NN-602	RT	70,000	92,500	ES	28	64
NN-603	RT	69,375	92,500	11	29	61
NN-606	RT	68,750	91,875	16	16	62
Mean	RT	69,375	92,290	13.5	24.3	62.3
Std dev'n		625	360	3.5	7.2	1.5
NN-609	580	63,125	90,625	10	22	51
NN-610	580	64,375	90,625	10	24	60
NN-616	580	64,370	90,625	10	23	58
Mean	580	63,950	90,625	10.0	23.0	56.3
Std dev'n		720	0	0	1.0	4.7

ES = Extensiometer slipped.

Table B-2. Preirradiation Tensile Properties of Shell Plate Material, HAZ, Heat C-4344-1

Specimen No.	Test temp, F	Strength, psi		Elongation, %		Red'n of area, %
		Yield	Ult.	Unif.	Total	
<u>Longitudinal</u>						
NN-501	RT	70,000	92,500	10	29	69
NN-502	RT	69,375	92,500	10	28	69
NN-503	RT	67,500	89,375	ES	28	70
Mean	RT	68,960	91,460	10.0	28.3	69.3
Std dev'n		1,300	1,805	0	0.6	0.6
NN-505	580	62,500	88,750	10	27	63
NN-506	580	61,250	88,750	14	26	60
NN-507	580	61,200	88,750	10	24	65
Mean	580	61,650	88,750	11.3	25.6	62.6
Std dev'n		740	0	2.3	1.5	2.5
<u>Transverse</u>						
NN-301	RT	69,375	91,875	9	22	63
NN-302	RT	70,000	91,875	8	23	65
NN-303	RT	68,750	91,875	10	22	62
Mean	RT	69,375	91,875	9.0	22.3	63.3
Std dev'n		625	0	1.0	0.6	1.5
NN-304	580	63,750	85,000	8	17	56
NN-305	580	63,125	86,875	9	18	57
NN-306	580	62,500	86,250	9	17	54
Mean	580	63,125	86,040	8.6	17.3	55.6
Std dev'n		625	955	0.6	0.6	1.5

ES = Extensiometer slipped.



Table B-3. Preirradiation Tensile Properties of Weld Metal, WF-209-1, Longitudinal

Specimen No.	Test temp, F	Strength, psi		Elongation, %		Red'n of area, %
		Yield	Ult.	Unif.	Total	
PP-015	RT	75,625	92,500	ES	28	64
PP-016	RT	78,125	95,000	12	28	62
PP-019	RT	77,500	94,063	12	31	62
Mean	RT	77,080	93,855	12	29.0	62.6
Std dev'n		1,300	1,260	0	1.7	1.1
PP-008	580	69,375	90,000	12	21	50
PP-009	580	66,250	87,500	12	22	53
PP-013	580	66,875	88,125	10	17	43
Mean	580	67,500	88,540	11.3	20.0	48.6
Std dev'n		1,650	1,300	1.1	2.6	5.1

ES = Extensiometer slipped.

APPENDIX C  
Preirradiation Charpy Impact Data

Table C-1. Preirradiation Charpy Impact Data for Shell Plate Material - Longitudinal Direction, Heat C-4344-1

Specimen No.	Test temp, F	Absorbed energy, ft-lb	Lateral expansion, $10^{-3}$ in.	Shear fracture, %
NN-805	-20	40	35	10
NN-809	-10	41	33	10
NN-803	0	39	34	20
NN-817	10	41	34	20
NN-818	15	57	46	30
NN-812	25	54	46	20
NN-802	55	12	10	10
NN-811	55	64	54	30
NN-804	70	77	55	40
NN-801	85	79	66	50
NN-813	90	102	75	80
NN-810	100	121	83	80
NN-814	120	116	84	80
NN-806	160	124	86	100
NN-815	330	121	90	100

Table C-2. Preirradiation Charpy Impact Data for Shell Plate  
Material - Transverse Direction, Heat C-4344-1

Specimen No.	Test temp, F	Absorbed energy, ft-lb	Lateral expansion, $10^{-3}$ in.	Shear fracture, %
NN-631	-20	20	18	0
NN-621	0	24	22	10
NN-683	20	34	30	10
NN-682	40	37	34	20
NN-619	60	50	47	20
NN-663	80	59	53	40
NN-680	100	68	60	50
NN-654	110	69	58	50
NN-611	125	73	64	80
NN-671	140	81	72	100
NN-684	155	93	81	100
NN-679	175	95	79	100
NN-659	200	92	74	100
NN-686	260	95	79	100
NN-603	325	93	78	100

Table C-3. Preirradiation Charpy Impact Data for Shell Plate  
Material - HAZ, Longitudinal Direction, Heat C-4344-1

<u>Specimen No.</u>	<u>Test temp, No.</u>	<u>Absorbed energy, ft-lb</u>	<u>Lateral expansion, 10<sup>-3</sup> in.</u>	<u>Shear fracture, %</u>
NN-516	-40	41	30	30
NN-507	-20	27	21	20
NN-504	0	48	41	40
NN-503	40	60	46	55
NN-513	60	65	52	90
NN-511	80	59	44	65
NN-501	90	77	62	70
NN-512	100	82	62	100
NN-506	140	102	73	100
NN-509	170	87	71	100
NN-505	200	93	73	100
NN-510	260	96	69	100
NN-508	320	89	70	100

Table C-4. Preirradiation Charpy Impact Data for Shell Plate  
Material - HAZ, Transverse Direction, Heat C-4344-1

Specimen No.	Test temp, F	Absorbed energy, ft-lb	Lateral expansion, $10^{-3}$ in.	Shear fracture, %
NN-331	-60	16	13	10
NN-304	-40	16	14	20
NN-308	-20	31	28	30
NN-309	0	38	34	30
NN-334	20	55	41	60
NN-313	40	43	42	50
NN-336	60	51	43	100
NN-326	80	67	57	100
NN-324	100	53	50	100
NN-343	110	60	55	100
NN-342	140	83	67	100
NN-305	170	86	73	100
NN-307	200	75	63	100
NN-332	260	77	63	100
NN-302	330	87	73	100

Table C-5. Preirradiation Charpy Impact Data for Weld Metal

<u>Specimen No.</u>	<u>Test temp, F</u>	<u>Absorbed energy, ft-lb</u>	<u>Lateral expansion, 10<sup>-3</sup> in.</u>	<u>Shear fracture, %</u>
PP-047	0	21	20	20
PP-050	15	27	26	30
PP-030	30	31	34	30
PP-042	40	34	32	30
PP-023	55	30	30	30
PP-027	75	36	36	40
PP-048	90	44	46	100
PP-040	105	46	45	100
PP-009	120	56	63	100
PP-012	135	39	42	100
PP-013	150	63	72	100
PP-025	200	68	69	100
PP-045	230	78	77	100
PP-020	260	79	77	100
PP-019	300	79	78	100

Figure C-1. Charpy Impact Data From Unirradiated Base Metal, Longitudinal Orientation

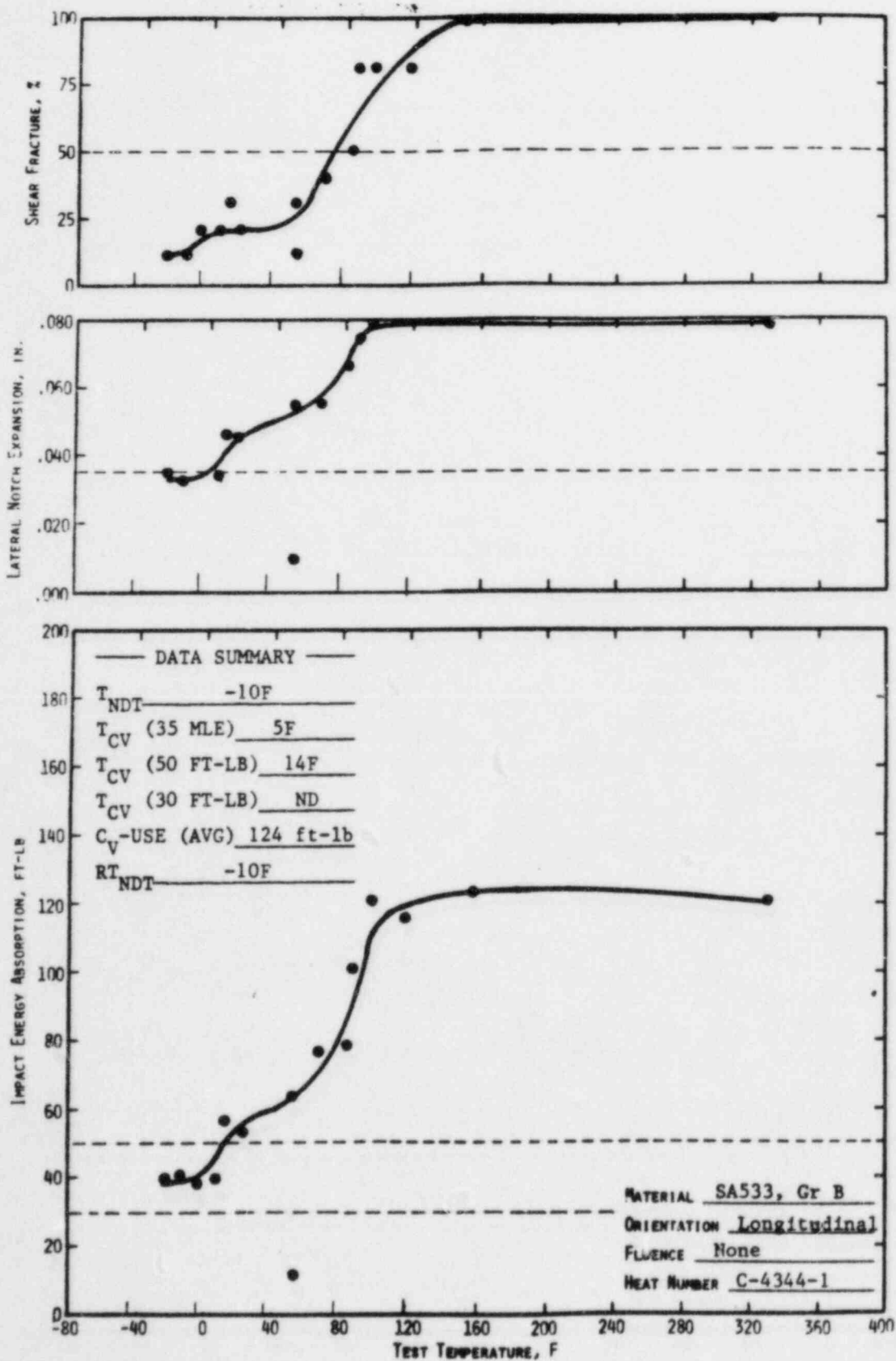




Figure C-2. Charpy Impact Data From Unirradiated Base Metal, Transverse Orientation

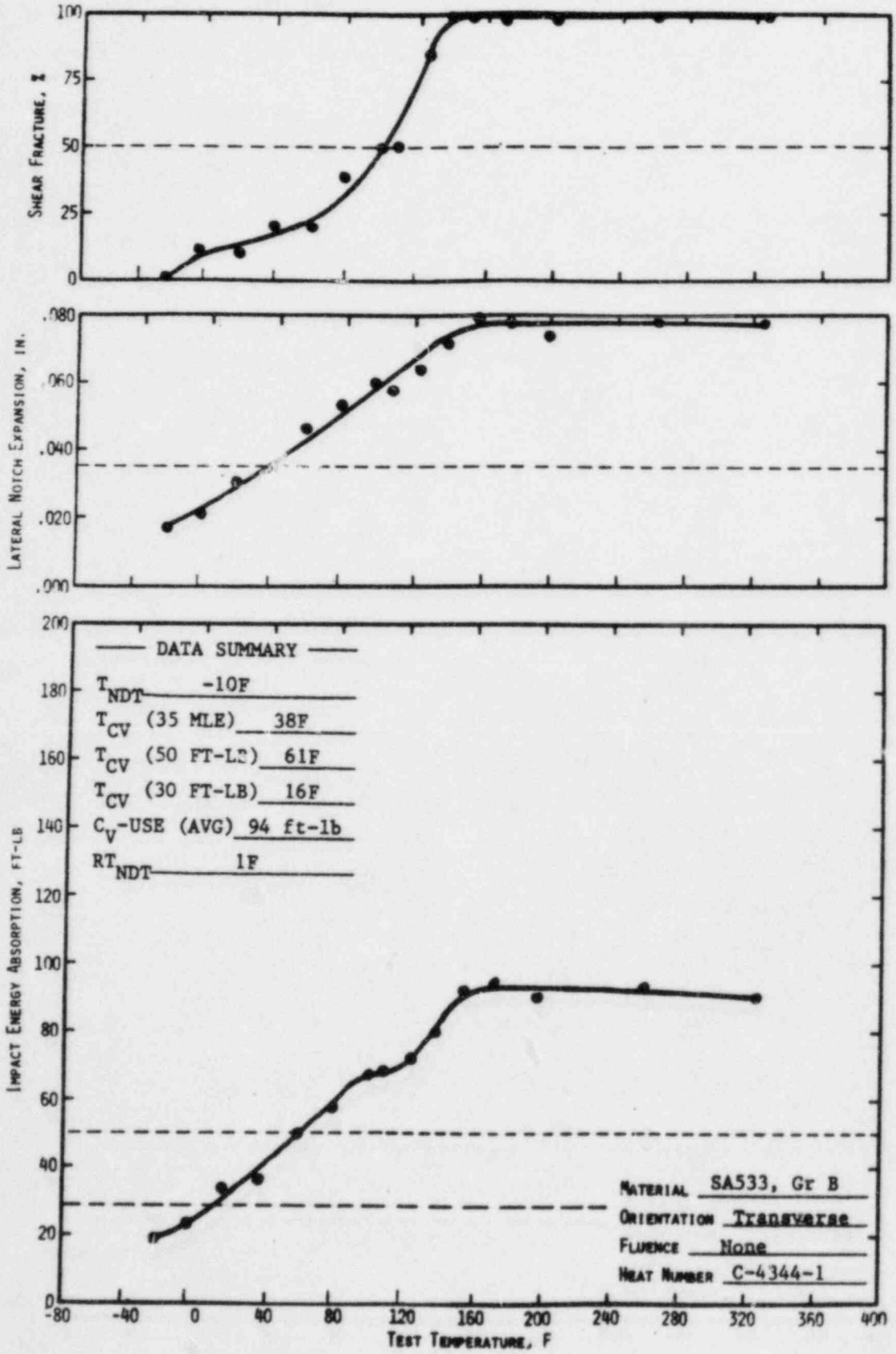


Figure C-3. Charpy Impact Data From Unirradiated Heat-Affected Zone Base Metal, Longitudinal Orientation

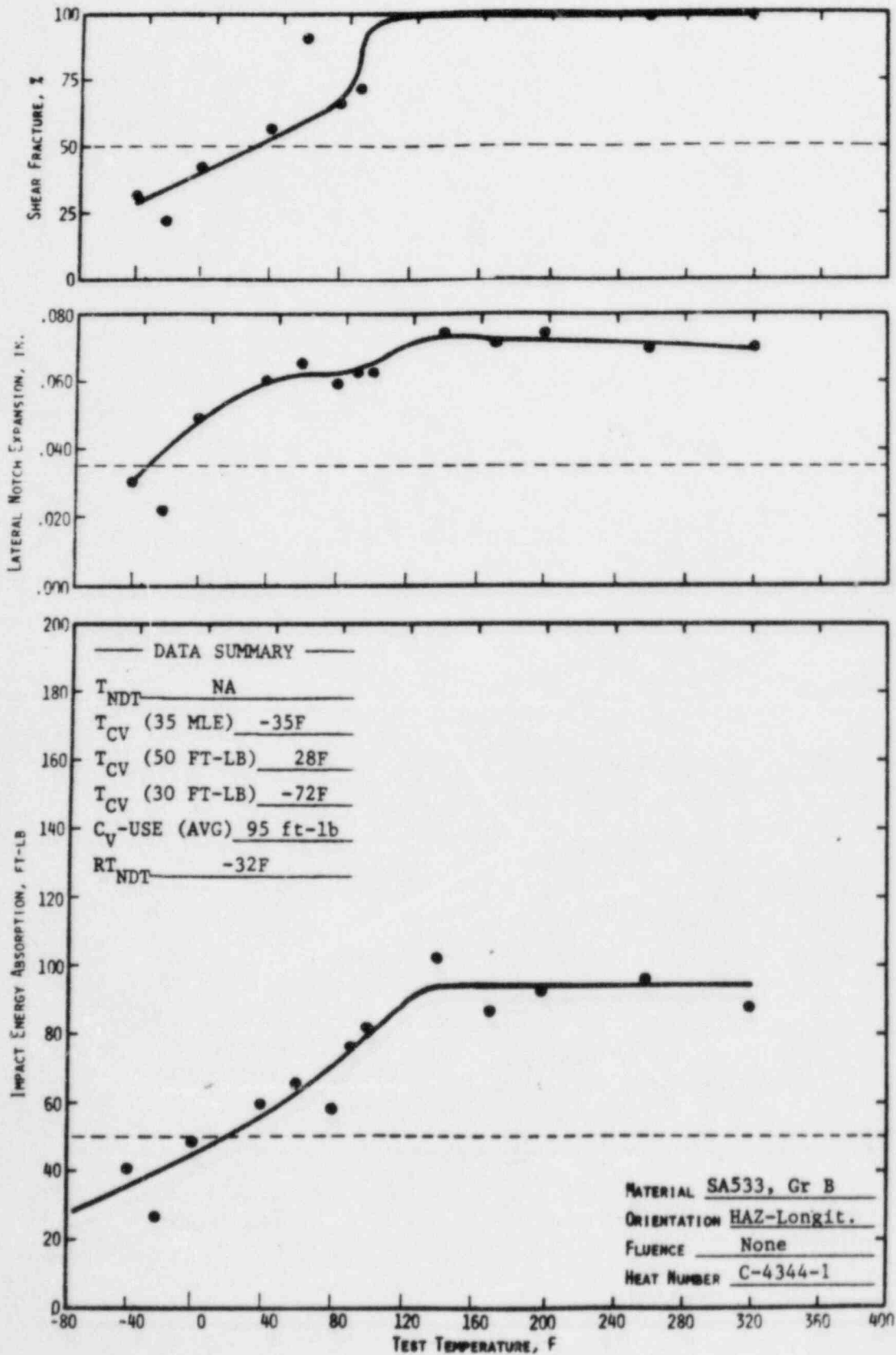


Figure C-4. Charpy Impact Data From Unirradiated Heat-Affected Zone Base Metal, Transverse Orientation

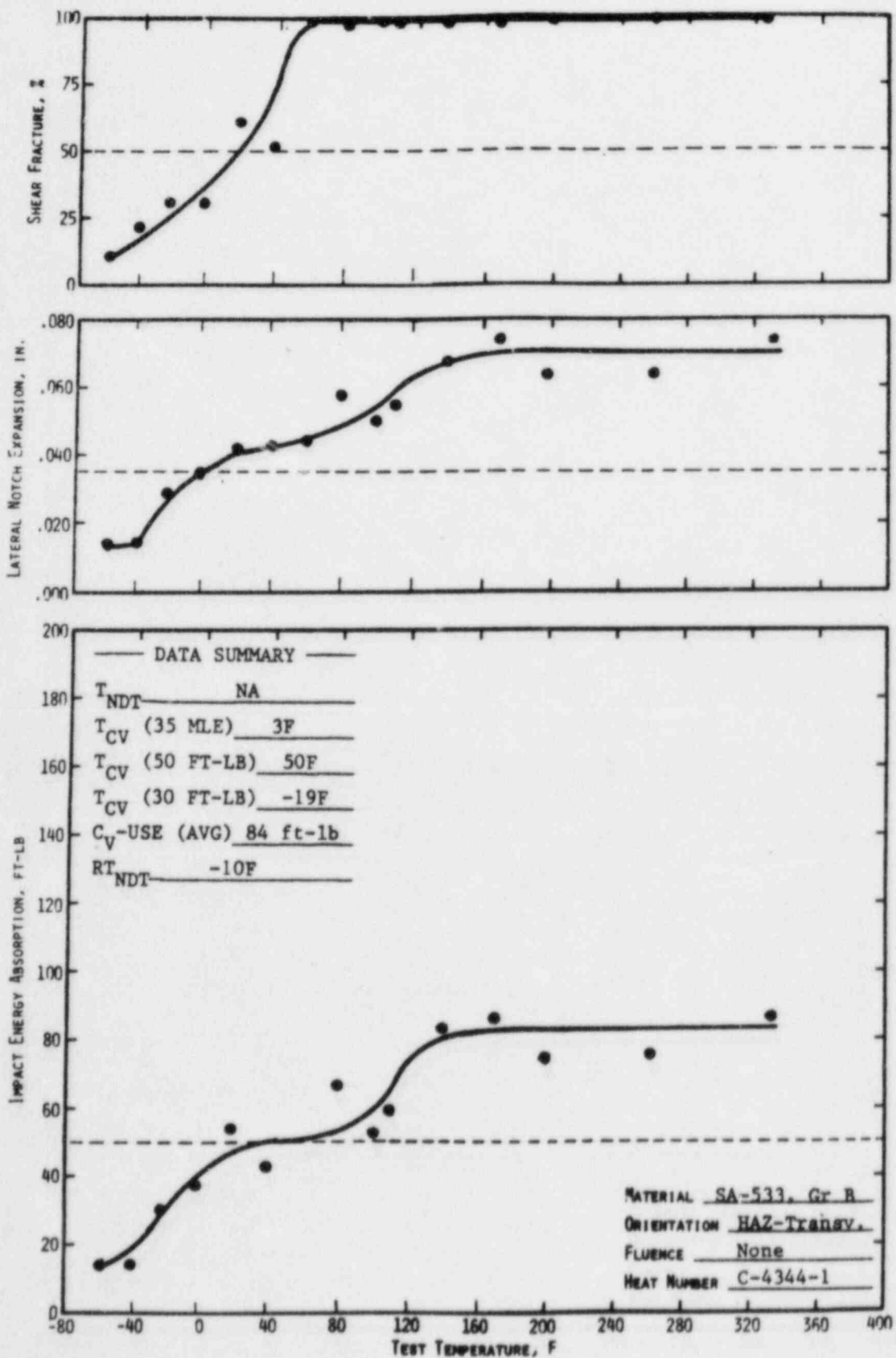
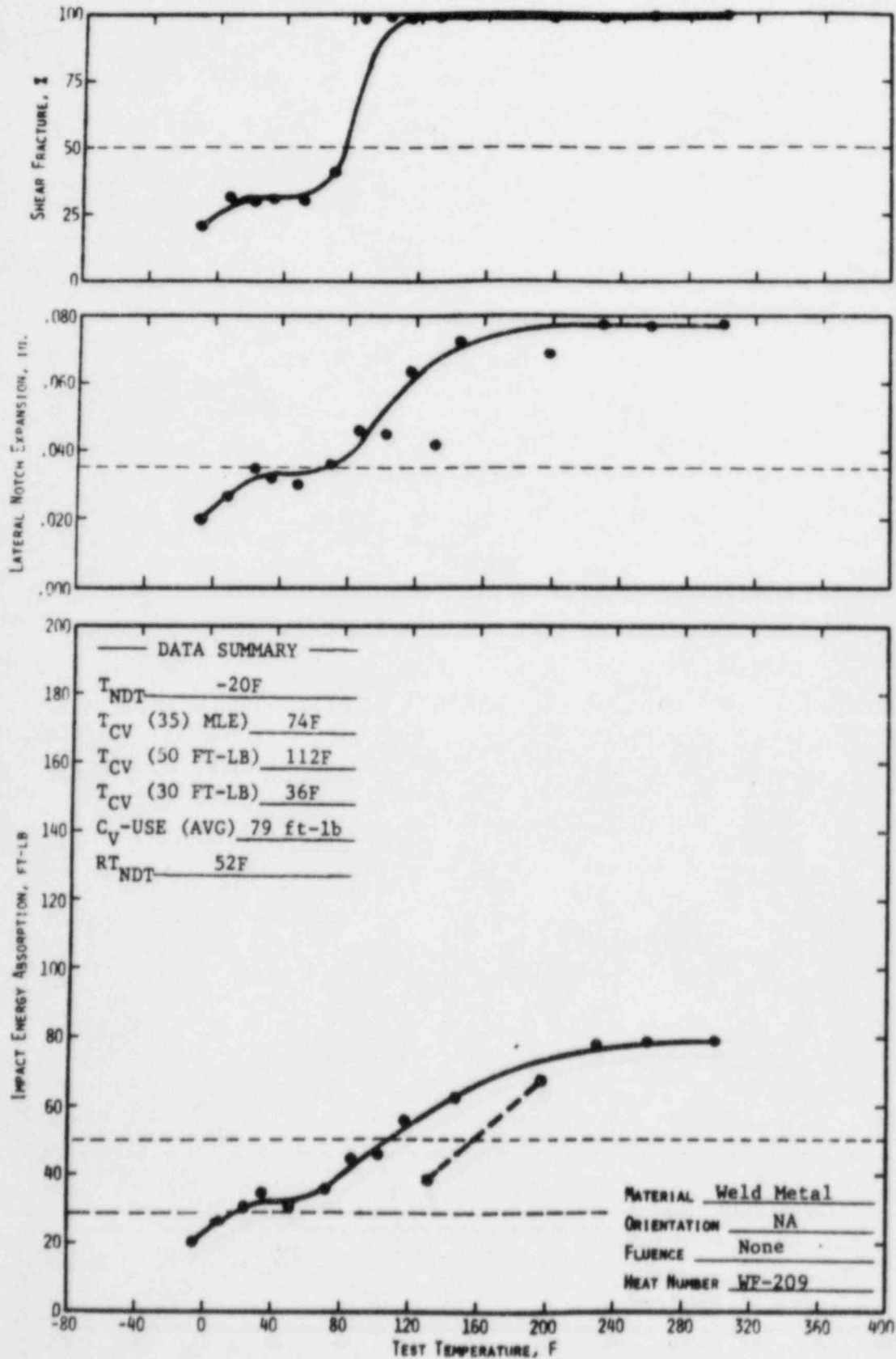


Figure C-5. Charpy Impact Data From Unirradiated Weld Metal



APPENDIX D  
Threshold Detector Information

Table D-1 lists the composition of the threshold detectors and the thickness of cadmium used to reduce competing thermal reactions. Table D-2 shows the cycle 1 measured activity per gram of target material (i.e., per gram of uranium, nickel, etc.) corrected for the wait time between irradiation and counting. Activation cross sections for the various materials were flux weighted with a  $^{235}\text{U}$  spectrum (Table D-3).

Table D-1. Detector Composition and Shielding

<u>Monitors</u>	<u>Shielding</u>	<u>Reaction</u>
10.38 wt % U-Al	Cd-Ag 0.02676 in. Cd	$^{238}\text{U}(n,f)$
1.61 wt % Np-Al	Cd-Ag 0.02676 in. Cd	$^{237}\text{Np}(n,f)$
Ni	Cd-Ag 0.02676 in. Cd	$^{58}\text{Ni}(n,p)^{58}\text{Co}$
0.56 wt % Co-Al	Cd-0.040 in. Cd	$^{59}\text{Co}(n,\gamma)^{60}\text{Co}$
0.56 wt % Co-Al	None	$^{59}\text{Co}(n,\gamma)^{60}\text{Co}$
Fe	None	$^{54}\text{Fe}(n,p)^{54}\text{Mn}$

Table D-2. Crystal River 3 Cycle 1 Neutron Dosimeters  
(Irradiation Ended March 3, 1978)

<u>Monitor material</u>	<u>Wt, gm</u>	<u>Reaction</u>	<u>Nuclide</u>	<u>Nuclide activity, <math>\mu</math>Ci</u>	<u><math>\mu</math>Ci/gm of material<sup>(a)</sup></u>	<u><math>\mu</math>Ci/gm of target<sup>(b,c)</sup></u>
<u>Set BD-1</u>						
$^{238}\text{U-A1}$	0.0800	$^{238}\text{U}(n,f)\text{Fp}$	$^{95}\text{Zr}$	0.414	5.18	50.3
			$^{103}\text{Ru}$	0.477	5.96	57.8
			$^{106}\text{Ru}$	0.0904	1.13	11.0
			$^{137}\text{Cs}$	0.0105	0.131	1.27
			$^{141}\text{Ce}$	0.413	5.16	50.1
			$^{144}\text{Ce}$	0.202	2.53	24.6
$^{237}\text{Np-A1}$	0.0566	$^{237}\text{Np}(n,f)\text{Fp}$	$^{95}\text{Zr}$	0.212	3.74	260
			$^{103}\text{Ru}$	0.225	3.98	276
			$^{106}\text{Ru}$	0.0371	0.656	45.6
			$^{137}\text{Ce}$	0.00461	0.0815	5.66
			$^{144}\text{Ce}$	0.0860	1.52	106
N1	0.133	$^{58}\text{Ni}(n,p)^{58}\text{Co}$	$^{58}\text{Co}$	98.0	737	1,090
		$^{60}\text{Ni}(n,p)^{60}\text{Co}$	$^{60}\text{Co}$	0.141	1.06	4.05
Co-A1 (5/8 in.) in Cd	0.0189	$^{59}\text{Co}(n,\gamma)^{60}\text{Co}$	$^{60}\text{Co}$	1.45	76.8	13,700
Co-A1 (1/2 in.)	0.0151	$^{59}\text{Co}(n,\gamma)^{60}\text{Co}$	$^{60}\text{Co}$	6.28	416	74,300
Fe	0.156	$^{54}\text{Fe}(n,p)^{54}\text{Mn}$	$^{54}\text{Mn}$	4.35	27.9	479
		$^{58}\text{Fe}(n,\gamma)^{59}\text{Fe}$	$^{59}\text{Fe}$	11.9	76.5	23,200

Table D-2. (Cont'd)

<u>Monitor material</u>	<u>Wt, gm</u>	<u>Reaction</u>	<u>Nuclide</u>	<u>Nuclide activity, <math>\mu</math>Ci</u>	<u><math>\mu</math>Ci/gm of material<sup>(a)</sup></u>	<u><math>\mu</math>Ci/gm of target<sup>(b,c)</sup></u>
<u>Set BD-2</u>						
<sup>238</sup> U-Al	0.0766	<sup>238</sup> U(n,f)Fp	<sup>95</sup> Zr	0.367	4.79	46.5
			<sup>103</sup> Ru	0.433	5.65	54.8
			<sup>106</sup> Ru	0.0715	0.933	9.05
			<sup>137</sup> Cs	0.00988	0.129	1.25
			<sup>141</sup> Ce	0.363	4.74	46.0
			<sup>144</sup> Ce	0.167	2.18	21.2
<sup>237</sup> Np-Al	0.0541	<sup>237</sup> Np(n,f)Fp	<sup>95</sup> Zr	0.233	4.31	299
			<sup>103</sup> Ru	0.234	4.33	301
			<sup>106</sup> Ru	0.0381	0.704	48.9
			<sup>137</sup> Cs	0.00539	0.0996	6.92
			<sup>144</sup> Ce	0.100	1.85	128
Ni	0.132	<sup>58</sup> Ni(n,p) <sup>58</sup> Co	<sup>58</sup> Co	93.5	708	1,040
		<sup>60</sup> Ni(n,p) <sup>60</sup> Co	<sup>60</sup> Co	0.136	1.03	3.94
Co-Al (5/8 in.) in Cd	0.0190	<sup>59</sup> Co(n, $\gamma$ ) <sup>60</sup> Co	<sup>60</sup> Co	7.01	74.7	13,300
Co-Al (1/2 in.)	0.0155	<sup>59</sup> Co(n, $\gamma$ ) <sup>60</sup> Co	<sup>60</sup> Co	1.16	369	65,900
Fe	0.154	<sup>54</sup> Fe(n,p) <sup>54</sup> Mn	<sup>54</sup> Mn	3.96	25.7	442
		<sup>58</sup> Fe(n, $\gamma$ ) <sup>59</sup> Fe	<sup>59</sup> Fe	10.3	67.2	20,400



Table D-2. (Cont'd)

<u>Monitor material</u>	<u>Wt, gm</u>	<u>Reaction</u>	<u>Nuclide</u>	<u>Nuclide activity, <math>\mu</math>Ci</u>	<u><math>\mu</math>Ci/gm of material<sup>(a)</sup></u>	<u><math>\mu</math>Ci/gm of target<sup>(b,c)</sup></u>
<u>Set HD-3</u>						
$^{238}\text{U}$ -Al	0.0792	$^{238}\text{U}(n,f)\text{Fp}$	$^{95}\text{Zr}$	0.367	4.63	44.9
			$^{103}\text{Ru}$	0.588	7.43	72.1
			$^{106}\text{Ru}$	0.108	1.36	13.2
			$^{137}\text{Cs}$	0.0116	0.147	1.43
			$^{141}\text{Ce}$	0.501	6.33	61.4
			$^{144}\text{Ce}$	0.247	3.12	30.3
			$^{237}\text{Np}$ -Al	0.0528	$^{237}\text{Np}(n,f)\text{Fp}$	$^{95}\text{Zr}$
$^{103}\text{Ru}$	0.317	6.01				417
$^{106}\text{Ru}$	0.0491	0.929				64.5
$^{137}\text{Cs}$	0.00713	0.135				9.38
$^{144}\text{Ce}$	0.120	2.28				158
Ni	0.133	$^{58}\text{Ni}(n,p)^{58}\text{Co}$	$^{58}\text{Co}$	118	887	1,310
		$^{60}\text{Ni}(n,p)^{60}\text{Co}$	$^{60}\text{Co}$	0.162	1.22	4.66
Co-Al (5/8 in.) in Cd	0.0191	$^{59}\text{Co}(n,\gamma)^{60}\text{Co}$	$^{60}\text{Co}$	1.22	98.3	17,600
Co-Al (1/2 in.)	0.0151	$^{59}\text{Co}(n,\gamma)^{60}\text{Co}$	$^{60}\text{Co}$	0.197	482	86,100
Fe	0.154	$^{54}\text{Fe}(n,p)^{54}\text{Mn}$	$^{54}\text{Mn}$	4.99	32.4	557
		$^{56}\text{Fe}(n,\gamma)^{59}\text{Fe}$	$^{59}\text{Fe}$	13.6	88.1	26,700

Table D-2. (Cont'd)

<u>Monitor material</u>	<u>Wt, gm</u>	<u>Reaction</u>	<u>Nuclide</u>	<u>Nuclide activity, <math>\mu</math>Ci</u>	<u><math>\mu</math>Ci/gm of material<sup>(a)</sup></u>	<u><math>\mu</math>Ci/gm of target<sup>(b,c)</sup></u>
<u>Set BD-4</u>						
$^{238}\text{U}$ -Al	0.0480	$^{238}\text{U}(n,f)\text{Fp}$	$^{95}\text{Zr}$	0.177	3.68	35.7
			$^{103}\text{Ru}$	0.222	4.63	44.9
			$^{106}\text{Ru}$	0.0391	0.814	7.90
			$^{137}\text{Cs}$	0.00445	0.0928	0.901
			$^{141}\text{Ce}$	0.177	3.68	35.7
			$^{144}\text{Ce}$	0.0787	1.64	15.9
$^{237}\text{Np}$ -Al	0.0752	$^{237}\text{Np}(n,f)\text{Fp}$	$^{95}\text{Zr}$	0.252	3.35	233
			$^{103}\text{Ru}$	0.271	3.61	251
			$^{106}\text{Ru}$	0.0411	0.547	38.0
			$^{137}\text{Cs}$	0.00605	0.0804	5.58
			$^{144}\text{Ce}$	0.103	1.37	95.1
Ni	0.139	$^{58}\text{Ni}(n,p)^{58}\text{Co}$	$^{58}\text{Co}$	73.7	530	782
		$^{60}\text{Ni}(n,p)^{60}\text{Co}$	$^{60}\text{Co}$	0.105	0.757	2.89
Co-Al (5/8 in.) in Cd	0.0195	$^{59}\text{Co}(n,\gamma)^{60}\text{Co}$	$^{60}\text{Co}$	0.710	49.6	8,860
Co-Al (1/2 in.)	0.0155	$^{59}\text{Co}(n,\gamma)^{60}\text{Co}$	$^{60}\text{Co}$	0.107	262	46,800
Fe	0.159	$^{54}\text{Fe}(n,p)^{54}\text{Mn}$	$^{54}\text{Mn}$	3.12	19.6	337
		$^{58}\text{Fe}(n,\gamma)^{59}\text{Fe}$	$^{59}\text{Fe}$	7.54	47.4	14,400

Table D-2. (Cont'd)

- (a) These data are the disintegration rates per gram of wire.
- (b) These data are the disintegration rates per gram of target nuclide; viz.,  $^{238}\text{U}$ ,  $^{237}\text{Np}$ ,  $^{58}\text{Ni}$ ,  $^{60}\text{Ni}$ ,  $^{59}\text{Co}$ ,  $^{54}\text{Fe}$ , and  $^{58}\text{Fe}$ .
- (c) The following abundances and weight percents were used to calculate the disintegration rate per gram of target element:
- $^{238}\text{U}$  - 10.38 wt %; 99.27% target nuclide
  - $^{237}\text{Np}$  - 1.44 wt %; 100% target nuclide
  - Ni - 100 wt %; 67.77%  $^{58}\text{Ni}$  target nuclide, 26.16%  $^{60}\text{Ni}$  target nuclide
  - Co - 0.56 wt %; 100%  $^{59}\text{Co}$  target nuclide
  - Fe - 100 wt %; 5.82%  $^{54}\text{Fe}$  target nuclide, 0.33%  $^{58}\text{Fe}$  target nuclide.

Table D-3. Dosimeter Activation Cross Sections<sup>(a)</sup>

<u>G</u>	<u>Energy range,</u> <u>MeV</u>	<u><sup>237</sup>Np</u>	<u><sup>238</sup>U</u>	<u><sup>58</sup>Ni</u>	<u><sup>54</sup>Fe</u>
1	13.3-15.0	2.321	1.073	0.4598	0.425
2	10.0-12.2	2.340	0.981	0.622	0.537
3	8.18-10.0	2.308	0.991	0.659	0.583
4	6.36-8.18	2.09	0.9165	0.638	0.572
5	4.96-6.36	1.54	0.600	0.540	0.473
6	4.06-4.96	1.533	0.562	0.403	0.325
7	3.01-4.06	1.616	0.553	0.264	0.206
8	2.46-3.01	1.691	0.550	0.139	0.096
9	2.35-2.46	1.695	0.553	0.089	0.0524
10	1.83-2.35	1.676	0.535	0.051	0.022
11	1.11-1.83	1.593	0.229	0.0128	0.0115
12	0.55-1.11	1.217	0.008	0.00048	--
13	0.111-0.55	0.1946	0.00013	--	--
14	0.0033-0.111	0.0410	--	--	--

(a) ENDF/4 values flux weighted with a fission spectrum from memo, L. A. Hassler to Distribution, "Documentation for Constants and Procedures used to Calculate Dosimeter Activities for RVSP Capsules," LR-845-7854-06, November 27, 1978.

CONTENTS

	Page
1. INTRODUCTION . . . . .	1-1
2. BACKGROUND . . . . .	2-1
3. SURVEILLANCE PROGRAM DESCRIPTION . . . . .	3-1
4. PREIRRADIATION TESTS . . . . .	4-1
4.1. Tensile Tests . . . . .	4-1
4.2. Impact Tests . . . . .	4-1
4.3. Compact Fracture Tests . . . . .	4-2
5. POST-IRRADIATION TESTS . . . . .	5-1
5.1. Thermal Monitors . . . . .	5-1
5.2. Tensile Test Results . . . . .	5-1
5.3. Charpy V-Notch Impact Test Results . . . . .	5-1
6. NEUTRON DOSIMETRY . . . . .	6-1
6.1. Introduction . . . . .	6-1
6.2. Analytical Approach . . . . .	6-2
6.3. Results . . . . .	6-3
6.4. Summary of Results . . . . .	6-4
7. DISCUSSION OF CAPSULE RESULTS . . . . .	7-1
7.1. Preirradiation Property Data . . . . .	7-1
7.2. Irradiated Property Data . . . . .	7-1
7.2.1. Tensile Properties . . . . .	7-1
7.2.2. Impact Properties . . . . .	7-1
8. DETERMINATION OF RCPB PRESSURE-TEMPERATURE LIMITS . . . . .	8-1
9. SUMMARY OF RESULTS . . . . .	9-1
10. SURVEILLANCE CAPSULE REMOVAL SCHEDULE . . . . .	10-1
11. CERTIFICATION . . . . .	11-1
12. REFERENCES . . . . .	12-1

CONTENTS (Cont'd)

	Page
<b>APPENDIX</b>	
A. Reactor Vessel Surveillance Program — Background Data and Information . . . . .	A-1
B. Preirradiation Tensile Data . . . . .	B-1
C. Preirradiation Charpy Impact Data . . . . .	C-1
D. Threshold Detector Information . . . . .	D-1

List of Tables

## Table

3-1. Specimens in Surveillance Capsule CR3-B . . . . .	3-2
3-2. Chemistry and Heat Treatment of Surveillance Materials . . . . .	3-3
5-1. Tensile Properties of Capsule CR3-B Base Metal and Weld Metal Irradiated to 1.0E18 nvt . . . . .	5-2
5-2. Charpy Impact Data From Capsule CR3-B Base Metal Irradiated to 1.0E18 . . . . .	5-2
5-3. Charpy Impact Data From Capsule CR3-B Heat-Affected Zone Metal Irradiated to 8.4E17 . . . . .	5-3
5-4. Charpy Impact Data From Capsule CR3-B Weld Metal Irradiated to 1.17E18 n/cm <sup>2</sup> . . . . .	5-3
6-1. Surveillance Capsule Detectors . . . . .	6-5
6-2. Dosimeter Activations . . . . .	6-5
6-3. Normalized Flux Spectra, Flux per MeV for Range . . . . .	6-6
6-4. Neutron Fluence . . . . .	6-6
6-5. Predicted Fast Fluence in Pressure Vessel at Maximum Location . . . . .	6-7
6-6. Calculated Neutron Fluence for Material Specimens . . . . .	6-7
7-1. Comparison of Tensile Test Results . . . . .	7-4
7-2. Observed Vs Predicted Changes in Irradiated Charpy Impact Properties . . . . .	7-5
8-1. Data for Preparation of Pressure-Temperature Limit Curves for Crystal River Unit 3, Applicable Through 8 EPFY . . . . .	8-4
A-1. Unirradiated Impact Properties and Residual Element Content Data of Beltline Region Materials Used for Selection of Surveillance Program Materials — Crystal River Unit 3 . . . . .	A-3
A-2. Test Specimens for Determining Material Baseline Properties . . . . .	A-4
A-3. Specimens in Upper Surveillance Capsules . . . . .	A-5
A-4. Specimens in Lower Surveillance Capsules . . . . .	A-5
B-1. Preirradiation Tensile Properties of Shell Plate Material, Heat C-4344-1 . . . . .	B-2
B-2. Preirradiation Tensile Properties of Shell Plate Materials, HAZ, Heat C-4344-1 . . . . .	B-3
B-3. Preirradiation Tensile Properties of Weld Metal, WF-209-1, Longitudinal . . . . .	B-4
C-1. Preirradiation Charpy Impact Data for Shell Plate Material — Longitudinal Direction, Heat C-4344-1 . . . . .	C-2

Table (Cont'd)

Table	Page
C-2. Preirradiation Charpy Impact Data for Shell Plate Material - Transverse Direction, Heat C-4344-1 . . . . .	C-3
C-3. Preirradiation Charpy Impact Data for Shell Plate Material - HAZ, Longitudinal Direction, Heat C-4344-1 . . . . .	C-4
C-4. Preirradiation Charpy Impact Data for Shell Plate Material - HAZ, Transverse Direction, Heat C-4344-1 . . . . .	C-5
C-5. Preirradiation Charpy Impact Data for Weld Metal . . . . .	C-6
D-1. Detector Composition and Shielding . . . . .	D-2
D-2. Crystal River 3 Cycle 1 Neutron Dosimeters . . . . .	D-3
D-3. Dosimeter Activation Cross Sections . . . . .	D-8

List of Figures

Figure	Page
3-1. Reactor Vessel Cross Section . . . . .	3-4
5-1. Charpy Impact Data for Irradiated Base Metal, Transverse Direction . . . . .	5-4
5-2. Charpy Impact Data for Irradiated Base Metal, Heat- Affected Zone . . . . .	5-5
5-3. Charpy Impact Data for Irradiated Weld Metal . . . . .	5-6
6-1. Predicted Fast Neutron Fluence at Various Locations Through Reactor Vessel Wall for First 8 EFPY . . . . .	6-8   1
7-1. Irradiated Vs Unirradiated Charpy Impact Properties of Base Metal . . . . .	7-6
7-2. Irradiated Vs Unirradiated Charpy Impact Properties of Heat-Affected Zone Material . . . . .	7-7
7-3. Irradiated Vs Unirradiated Charpy Impact Properties of Weld Metal . . . . .	7-8
8-1. Fast Neutron Fluence of Surveillance Capsule Center Compared to Various Locations Through Reactor Vessel Wall for First 8 EFPY . . . . .	8-5   1
8-2. Reactor Vessel Pressure-Temperature Limit Curves for Normal Operation Heatup Applicable for First 8 EFPY . . . . .	8-6
8-3. Reactor Vessel Pressure-Temperature Limit Curve for Normal Operation - Cooldown Applicable for First 8 EFPY . . . . .	8-7
8-4. Reactor Vessel Pressure-Temperature Limit Curve for Inservice Leak and Hydrostatic Tests, Applicable for First 8 EFPY . . . . .	8-8
A-1. Location and Identification of Materials Used in Fabrication of Crystal River 3 Reactor Pressure Vessel . . . . .	A-6
A-2. Location of Longitudinal Welds in Upper and Lower Shell Courses . . . . .	A-7
A-3. Loading Diagram for Test Specimens in Lower Surveillance Capsule CR3-B . . . . .	A-8
C-1. Charpy Impact Data From Unirradiated Base Metal, Longitudinal Orientation . . . . .	C-7
C-2. Charpy Impact Data From Unirradiated Base Metal, Transverse Orientation . . . . .	C-8

Figures (Cont'd)

Figure	Page
C-3. Charpy Impact Data From Unirradiated Heat-Affected Zone Base Metal, Longitudinal Orientation . . . . .	C-9
C-4. Charpy Impact Data From Unirradiated Heat-Affected Zone Base Metal, Transverse Orientation . . . . .	C-10
C-5. Charpy Impact Data From Unirradiated Weld Metal . . . . .	C-11